

 Open access • Posted Content • DOI:10.1101/2020.05.20.105353

Glyphosate inhibits melanization and increases insect susceptibility to infection

— [Source link](#) 

Daniel F Q Smith, Emma Camacho, Raviraj Thakur, Alexander J. Barron ...+2 more authors

Institutions: Johns Hopkins University, University of Connecticut

Published on: 20 May 2020 - bioRxiv (Elsevier Limited)

Related papers:

- [Glyphosate inhibits melanization and increases susceptibility to infection in insects.](#)
- [Plant defenses interact with insect enteric bacteria by initiating a leaky gut syndrome](#)
- [Metabolomics reveals insect metabolic responses associated with fungal infection.](#)
- [Increase in midgut microbiota load induces an apparent immune priming and increases tolerance to *Bacillus thuringiensis*.](#)
- [Can Insects Develop Resistance to Insect Pathogenic Fungi](#)

Share this paper:    

View more about this paper here: <https://typeset.io/papers/glyphosate-inhibits-melanization-and-increases-insect-cg1xvytdz>

1 **Glyphosate Inhibits Melanization and Increases Susceptibility to Infection in Insects**

2

3 Daniel F. Q. Smith¹, Emma Camacho¹, Raviraj Thakur^{2†¶}, Alexander J. Barron^{3†}, Yuemei Dong¹,

4 George Dimopoulos¹, Nichole A. Broderick^{3Ω}, Arturo Casadevall^{1Ω*}

5

6 ¹Department of Molecular Microbiology and Immunology, Johns Hopkins Bloomberg School of

7 Public Health, ² Department of Otolaryngology, Head and Neck Surgery, Johns Hopkins

8 Medicine, Baltimore, MD 21205, ³ Department of Biology, Johns Hopkins University, Baltimore

9 MD 21218, United States of America.

10

11 Running title: Glyphosate Inhibits Melanization in Insects

12

*Correspondence: acasade1@jhu.edu

† Authors contributed equally

Ω N.A.B. and A.C. share senior authorship

¶ Current Address: Cancer Early Detection Advanced Research Center, Knight Cancer Institute, Oregon Health and Science University, Portland, OR 97201

13 **ABSTRACT**

14 Melanin, a black-brown pigment found throughout all kingdoms of life, has diverse
15 biological functions including: UV protection, thermoregulation, oxidant scavenging, arthropod
16 immunity, and microbial virulence. Given melanin's broad roles in the biosphere, particularly in
17 insect immune defenses, it is important to understand how exposure to ubiquitous
18 environmental contaminants affects melanization. Glyphosate – the most widely used herbicide
19 globally – inhibits melanin production, which could have wide-ranging implications in the health
20 of many organisms, including insects. Here, we demonstrate that glyphosate has deleterious
21 effects on insect health in two evolutionary distant species, *Galleria mellonella* (Lepidoptera:
22 Pyralidae) and *Anopheles gambiae* (Diptera: Culicidae), suggesting a broad effect in insects.
23 Glyphosate reduced survival of *G. mellonella* caterpillars following infection with the fungus
24 *Cryptococcus neoformans* and decreased the size of melanized nodules formed in hemolymph,
25 which normally help eliminate infection. Glyphosate also increased the burden of the malaria-
26 causing parasite *Plasmodium falciparum* in *A. gambiae* mosquitoes, altered uninfected
27 mosquito survival, and perturbed the microbial composition of adult mosquito midguts. Our
28 results show that glyphosate's mechanism of melanin inhibition involves antioxidant synergy
29 and disruption of the reaction oxidation-reduction balance Overall, these findings suggest that
30 glyphosate's environmental accumulation could render insects more susceptible to microbial
31 pathogens due to melanin inhibition, immune impairment, and perturbations in microbiota
32 composition, potentially contributing to declines in insect populations.

33

34 Key Words: melanin, phenoloxidase, malaria, midgut microbiome, microbiota *Galleria*
35 *mellonella*, *Anopheles*, vector biology, nodulation, fungi, tyrosinase, hormesis, antioxidant, acid
36 synergism

37

38 INTRODUCTION

39 Melanin, a black-brown pigment found in all biological kingdoms, is produced through a
40 series of oxidation and reduction reactions. These reactions are typically catalyzed by two
41 classes of enzymes: laccases (EC. 1.10.3.2) and phenoloxidases – a family which includes
42 tyrosinases (EC. 1.14.18.1) (1). Tyrosinases are copper metalloenzymes found in bacteria,
43 fungi, protists, arthropods, birds, and mammals (2–7), and have two catalytic roles: 1)
44 hydroxylation of monophenols into *ortho*-diphenols, followed by 2) oxidation of *o*-catechols into
45 *o*-quinones (8). During melanization, tyrosinase converts 3,4-dihydroxyphenylalanine (L-DOPA)
46 to dopaquinone. Dopaquinone undergoes oxidation and reduction reactions to first form
47 dopachrome, then dihydroxyindole. Dihydroxyindole undergoes radical-mediated polymerization
48 to form melanins (8,9).

49 Melanization is an important component of immunity in virtually all insects (9). Upon
50 infection, protease cascades are activated that cleave pro-phenoloxidases into active
51 phenoloxidases. Phenoloxidases convert catecholamines in the hemolymph into melanin, which
52 surrounds and eliminates the pathogen through exposure to reactive oxygen species (ROS) and
53 lysis from toxic melanin intermediates (3,9–13). This melanization process is a key component
54 of insect immune defense against bacterial, fungal, and protozoan pathogens, nematode
55 parasites, and insect parasitoids (14–21). In addition, pathogens are cleared by two similar
56 processes: nodulation of smaller microbes such as bacteria, fungi, and protozoa, and
57 encapsulation for infections with larger organisms such as helminths and parasitoid eggs (22).
58 Both nodulation and encapsulation involve pathogen neutralization via melanin accumulation
59 and hemocyte (insect “blood cells”) aggregation around the pathogen (22). Melanization and
60 phenoloxidases are also important for wound healing and cuticular development – processes
61 vital for insect health and survival (23,24). Since melanization is an essential physiological
62 process and effector of insect health, understanding how common environmental contaminants
63 affect melanin production is important. The significance of this is also highlighted by findings

64 suggesting that insect populations may be in decline in recent decades (25).

65 One ubiquitous chemical found in the environment is glyphosate, the most commonly
66 used herbicide world-wide, which was previously shown to interfere with melanization in the
67 fungus *Cryptococcus neoformans* (26). Glyphosate is a phosphonic glycine analogue and the
68 active ingredient in Roundup herbicides (27). It kills plants through competitive inhibition of
69 EPSP synthase in the shikimate pathway responsible for aromatic amino acid synthesis in many
70 plants, fungi, and bacteria (28). The low cost of glyphosate and wide availability of genetically-
71 modified glyphosate-resistant crops has increased both crop yields and glyphosate-based
72 herbicide use in agriculture (29,30). Between 1996-2014, glyphosate-resistant crops were linked
73 to a 12-fold global increase in glyphosate use, including 8-fold in the US, 134-fold in Brazil, and
74 107-fold in Argentina (31,32).

75 In practice, glyphosate is commonly applied at concentrations of ~28 to 57 mM (33) or in
76 formulations of 360 g/L (2 M), with 720 g (4 mol) per hectare (34). Glyphosate-based herbicides
77 are sprayed onto crops where the glyphosate is taken up by plant leaves and translocated to
78 growing tissues throughout the plant (35). Glyphosate is translocated to the roots where it is
79 released into the soil (34). In total, about 88% of the sprayed glyphosate ends up in the topsoil
80 (36–38)(38) . Less than 1% of glyphosate has been shown to enter water bodies, typically
81 following heavy rain, snowmelt, ploughing, or erosion (37), but concentrations from <1 nM to
82 ~30 µM in nearby water have been reported (39). Further, glyphosate has been shown to enter
83 the air through wind erosion and deposit via rain (40).

84 Glyphosate is remarkably stable, with half-life ranging from weeks to years depending
85 on the surrounding microbial populations, which provide the primary mechanism of glyphosate
86 degradation, while temperature, light, acidity, and salinity also play roles in the degradation
87 process. Microbes mostly break down glyphosate into aminomethylphosphonic acid (AMPA),
88 which persists up to 20 times longer than glyphosate, and is often found in higher
89 concentrations in topsoil and water (41–45).

90 While glyphosate may have harmful effects on microbes and animals (as reviewed in
91 (35,46)), its impact on environmental microbial communities is inconclusive. Some studies
92 demonstrate clear perturbation of microbial communities, including disrupting rhizosphere
93 composition and fungal endophyte growth and viability (47–50), while others show little to no
94 long term impact on microbial communities (51–53), with no effects on overall soil health or
95 reduction in soil microbial mass (54). Microbial communities are also abundant in insect guts,
96 where they are important for insect health (55–58), and several studies have linked detrimental
97 effects of glyphosate on insect health to disruption of the microbiota. Honeybees exposed to
98 glyphosate have altered microbiomes and are more susceptible to *Serratia marcescens* (59),
99 although AMPA did not have the same effect (60). In tsetse fly midguts, glyphosate disrupts
100 *Wigglesworthia glossinidia*'s production of folate - a compound required for tsetse fly health and
101 vector competence for *Trypanosoma brucei* parasites (61).

102 Beyond effects on microbial communities, glyphosate has broad physiological impacts
103 on insects, other arthropods, and vertebrates. While glyphosate was harmless to *Lepthyphantes*
104 *tenuis* spiders, it changed behavior and increased mortality in *Pardosa milvina* and *Neoscona*
105 *theisi* spiders (62–64). Glyphosate reduced learning in *Aedes aegypti* mosquitoes (65) and in
106 honeybees reduced survival and caused learning defects associated with feeding, homing, and
107 flight behaviors (66,67). Glyphosate and AMPA delayed development and reduced survival of
108 the arthropod *Daphnia magna* (68). Glyphosate induces oxidative stress and damage in many
109 organisms, including *D. magna*, insects (fruit flies), amphibians (African clawed frog, European
110 green toad, marsh frog), fish (brown trout, spotted snakehead fish), and mammals (rats) (69–
111 74), often linked with lipid peroxidation and expression of antioxidant defenses (catalase,
112 glutathione, and superoxide dismutase). In human erythrocytes, glyphosate and AMPA mixtures
113 increase ROS production (75,76).

114 Given the melanin-inhibitory properties of glyphosate in fungi (26), we examined the
115 roles of glyphosate and AMPA as inhibitors of insect melanization and phenoloxidase. We used

116 two distinct insect models that both rely on melanin-based immunity: *Galleria mellonella* – a
117 species of wax moths (Lepidoptera: Pyralidae), and *Anopheles gambiae* – a mosquito vector of
118 malaria (Diptera: Culicidae). Considering melanin’s importance in insect immunity, we evaluated
119 glyphosate’s effects on *G. mellonella* susceptibility to the pathogenic fungus *C. neoformans*, and
120 on *A. gambiae* survival and susceptibility to the malaria parasite *Plasmodium falciparum* as
121 measured by parasite oocyst burden. Additionally, we evaluated glyphosate’s mechanism of
122 melanin inhibition using L-DOPA auto-oxidation and mushroom tyrosinase-mediated oxidation
123 models. Mushroom tyrosinase is commercially available and produces melanin in a similar
124 mechanism as insect phenoloxidase. The purified enzyme and L-DOPA auto-oxidation allowed
125 us to take a controlled step-by-step biochemical approach to show that glyphosate inhibits
126 melanization by disrupting oxidative balance.

127

128 **RESULTS**

129 **Glyphosate and AMPA Inhibit *Galleria mellonella* Phenoloxidase Activity**

130 In insects, phenoloxidases are activated by serine proteases upon wounding or infection,
131 thus triggering melanin production to either clot a wound or restrict a pathogen (77). To
132 investigate whether glyphosate inhibited insect melanogenesis, we used two models: *G.*
133 *mellonella* wax moth larvae, and *A. gambiae* adult mosquitoes, a main vector of malaria.
134 In an *ex vivo* analysis using *G. mellonella* hemolymph, we found that glyphosate inhibited
135 phenoloxidase activity in a dose dependent manner, without addition of exogenous substrate
136 (Fig. 1A). Similar results were found with addition of a broad-spectrum protease inhibitor, which
137 was used to control for continued activation of phenoloxidase, glyphosate-induced cellular
138 responses, and/or off-target effects on other components of the phenoloxidase cascade
139 (Supplementary Fig. 1A). We also saw similar inhibition of phenoloxidase activity with the
140 addition of exogenous L-DOPA; however, in these experiments there was only a modest
141 enhancement of phenoloxidase activity with lower glyphosate concentrations followed by

142 striking inhibition at higher concentrations (Supplementary Fig 1B). Importantly, glyphosate did
143 not impact hemocyte viability, as measured by trypan blue exclusion (Supplementary Fig. 1C).
144 Aminomethylphosphonic acid (AMPA), a primary breakdown product of glyphosate that
145 accumulates in the environment (45), inhibited melanization similarly to glyphosate using *G.*
146 *mellonella* hemolymph and a commercially available mushroom tyrosinase (Fig. 1B,
147 Supplementary Fig 1D). These data show that glyphosate inhibits melanization in insects similar
148 to what has been previously shown in fungi (26), thus indicating that glyphosate interferes with
149 major melanin-based processes in at least two kingdoms of life.

150

151 **Glyphosate Alters *G. mellonella* Susceptibility to Infection**

152 Next, we sought to determine whether glyphosate increased *in vivo* susceptibility of
153 *Galleria mellonella* larvae to foreign organisms. We injected *G. mellonella* final instar larvae with
154 2 µg of glyphosate (~8-12 ng/mg per larvae) followed by infection with *C. neoformans* or a mock
155 infection. The two mock infected groups, glyphosate-treated and phosphate-buffered saline
156 (PBS)-treated exhibited similar survival. However, in the infected groups, the glyphosate-treated
157 larvae died faster compared to the PBS-treated controls (Gehan-Breslow-Wilcoxon test, $p =$
158 0.013) (Fig. 1C). A similar, but non-significant, trend was seen with a *C. neoformans lac1Δ*
159 strain (Supplementary Fig. 1E). The *lac1Δ* strain is unable to produce melanin, an important
160 virulence factor in *C. neoformans* pathogenesis. This strain is less virulent in the *G. mellonella*
161 model (78), potentially contributing to the lack of significant differences between the glyphosate
162 and PBS-treated groups.

163 The decreased survival of the glyphosate-treated group infected with *C. neoformans*
164 was correlated with smaller melanized particles within nodules formed during infection (*in vivo*),
165 as compared to the PBS-treated group infected with *C. neoformans* (Fig 1D). For these
166 experiments, we infected and drugged *G. mellonella* as we do during normal infections, then
167 collected the hemolymph 24 hours later and imaged the nodules and aggregates that formed *in*

168 *vivo*. The PBS-treated non-infected group had smaller or virtually no melanized structures. In
169 two of three replicates, the PBS-treated infected group had more melanized structures than the
170 glyphosate-treated group (Supplementary Fig 1G-I). Further, in the glyphosate-treated infected
171 group we observed more *C. neoformans* cells, and those within nodules displayed lower
172 degrees of melanin encapsulation compared to PBS-treated larvae (Chi-squared test, $p =$
173 0.0034) (Fig 1E). The scoring was based on a system devised with 0 representing no melanin
174 encapsulation of the yeast cell to 4 being the most melanin encapsulation, as depicted in (Fig
175 1F). The one-time treatment with glyphosate did not disrupt time to larval pupation, a process
176 mediated by laccases and phenoloxidases (Supplementary Fig. 1F). These data suggest a
177 direct correlation between glyphosate treatment, and increased susceptibility of *G. mellonella* to
178 infection caused by decreased melanin-based immune response (nodulation).

179

180 **Glyphosate Alters *A. gambiae* Phenoloxidases, Susceptibility to Infection with Malaria** 181 **Parasites, and Survival**

182 To ascertain the impact of glyphosate on *Anopheles gambiae* mosquito melanization,
183 we measured the phenoloxidase activity in whole-body mosquito homogenate following the
184 addition of glyphosate. Similar to our results with *G. mellonella*, glyphosate inhibited
185 phenoloxidase activity of *A. gambiae* homogenate in a dose-dependent manner (Fig. 2A).

186 To investigate whether glyphosate rendered mosquitoes more susceptible to infection
187 with the human malaria parasite *P. falciparum*, adult female mosquitoes were fed on 10% sugar
188 solution supplemented with glyphosate at different concentrations for 5 days and then given a *P.*
189 *falciparum*-infected blood meal. Parasite burden was assessed through enumeration of the
190 *Plasmodium* oocyst stage at 8 days post infection (DPI). Glyphosate-fed mosquitoes had higher
191 oocyst burdens with an overall non-significant trend of increasing oocyst burden with increasing
192 dose of glyphosate (Fig. 2B). However, we observed a sharp decline in parasite burden in the
193 10 mM treated group, which was likely due to the increased mortality of this group (Fig. 2C)

194 resulting in few surviving mosquitoes to assess the intensity of infection. In a low *P. falciparum*
195 infection intensity assay (Supplementary Fig. 2A), we observed that glyphosate-treated groups
196 are more likely to be infected than control groups. This is important, as lower parasite burdens
197 are more reminiscent of infections in field conditions in malaria endemic regions (79–82).

198 Sugar preparations with glyphosate at environmentally relevant concentrations were
199 given to *A. gambiae* mosquitoes to ascertain the herbicide's effect on the mosquito's lifespan.
200 Compared to control mosquitoes (sugar-fed without glyphosate), mosquitoes given low
201 glyphosate doses (30 to 300 μ M) showed statistically significant improved survival, while those
202 fed higher doses of glyphosate (1 to 10 mM) had equal or decreased survival, with the 10 mM
203 glyphosate-exposed group exhibiting significantly decreased survival (Fig. 2C). Additionally, we
204 used a Cox Mixed Effects Model to account for fixed and random effects, and calculated the
205 Hazard Ratios for each of the treatment groups (Fig. 2D). Hazard Ratios <1 indicate a reduced
206 risk of death compared to the control while Hazard Ratios >1 indicate enhanced risk of death
207 compared to the control group. With this model, the mosquitoes treated with lower glyphosate
208 concentrations had a Hazard Ratio less than 1, those treated with 1 and 3 mM glyphosate had
209 Hazard Ratios similar to 1, and the 10 mM-treated mosquitoes had a Hazard Ratio significantly
210 greater than 1. These results suggest that glyphosate could have bimodal effects on mosquito
211 health.

212 We also measured the impact of glyphosate on the mosquito cuticle and body size.
213 There was no discernable difference in *A. gambiae* cuticle pigmentation after 5 days of
214 treatment with 1 mM glyphosate in 10% sucrose from days 3 to 8 post-emergence, as
215 measured by mean gray value of the ventral abdomen (Supplementary Fig. 2C). This was
216 expected due to the typical expression of cuticular laccases being largely at the timing of
217 pupation and the first three days post-emergence (23,24). Additionally, there were no difference
218 in wing length, a proxy for adult size, between the glyphosate-treated and untreated adult
219 mosquitoes (Supplementary Fig. 2D). Altogether, this suggests that the observed increased

220 parasite burden in glyphosate-treated mosquitoes cannot be explained merely by broader
221 impacts of glyphosate on mosquito health.

222

223 **Glyphosate Alters the Composition, but Not Density, of the *A. gambiae* Midgut Microbiota**

224 *A. gambiae* midgut microbiota can influence *Plasmodium* infection by modulating the
225 mosquito's innate immune system and hence affecting parasite viability (83–86). We
226 investigated whether glyphosate had detrimental effects or influence on the *A. gambiae*
227 microbiota. Colony Forming Unit (CFU) counts from cultures of midgut homogenates grown on
228 LB agar demonstrated that glyphosate treatment did not affect total number of culturable gut
229 bacteria (Fig. 3A), though this method would miss any impacts on microbes that were not
230 readily cultured by these methods. To complement our culture-dependent analysis and provide
231 insight on microbiota community composition, we compared the total 16S rRNA composition of
232 the midgut microbiota with and without glyphosate treatment. Glyphosate treatment altered
233 microbiota composition, with a noted decrease in the relative abundance of Enterobacteriaceae
234 and an increase in relative *Asaia spp.* populations (Fig. 3B). We did not observe a dose-
235 dependent impact on composition, as the alpha diversity (a function of the number of bacterial
236 taxa) of mosquitoes exposed to glyphosate was similar to controls (Fig. 3C). However,
237 community composition was perturbed by treatment with glyphosate, and glyphosate-treated
238 groups and controls form two separate clusters in principal coordinates analysis as measured
239 by Bray-Curtis dissimilarity (Fig. 3D). These differences suggest a shift in beta diversity
240 (prevalence of each bacterial taxon), and therefore a difference between the microbial
241 communities of mosquitoes exposed to glyphosate versus untreated controls.

242

243 **Glyphosate Inhibits Production of Dopaquinone, Dopachrome, and Melanin**

244 To understand how glyphosate inhibited melanization, we evaluated the formation of
245 melanin intermediates in a stepwise manner using a commercially available fungal tyrosinase

246 and the melanin precursor L-DOPA (2 mM). Although this tyrosinase differs from insect
247 phenoloxidase, the melanization reaction in these systems follows the same Mason-Raper
248 pathway (Figure 4A) (87,88) and thus can be used to explore the mechanism of glyphosate
249 inhibition. The first step of the reaction involves L-DOPA oxidation to dopaquinone (DQ)
250 enzymatically or spontaneously (89). We found that glyphosate inhibited the dopaquinone
251 production in a dose-dependent manner (Fig. 4B). This inhibition was observed for both
252 tyrosinase-mediated and auto-oxidation-mediated production of dopaquinone. The slopes of
253 inhibition in the auto-oxidation and tyrosinase-mediated oxidation were similar. This indicated
254 that the tyrosinase reaction dopaquinone levels would remain unchanged by glyphosate
255 treatment if the inhibition of “background” auto-oxidation dopaquinone production were taken
256 into consideration. These results suggested that dopaquinone inhibition was primarily rooted in
257 preventing the oxidation of L-DOPA independent of tyrosinase.

258 Dopaquinone spontaneously cyclizes to form cyclodopa, which then undergoes a redox
259 exchange with another dopaquinone molecule to form one molecule of dopachrome and one
260 reformed molecule of L-DOPA. Dopachrome is a pink-orange melanin intermediate that has an
261 absorbance maximum at 475 nm. Dopachrome is a useful proxy product for tyrosinase-
262 mediated reaction kinetics and evaluating the melanization reactions and redox exchange (90).
263 The rate of dopachrome formation and the amount of dopachrome produced were determined
264 by measuring changes in absorbance during a reaction between L-DOPA and tyrosinase. There
265 was a strong dose-dependent inhibition of dopachrome formation with glyphosate (Fig. 4C),
266 implying that the compound’s inhibitory effects were upstream of dopachrome.

267 We tracked the reaction over 5 d to confirm inhibition of melanin synthesis. Glyphosate
268 inhibited the production of a black pigment dose-dependently, as measured by the absorbance
269 of the tyrosinase reaction on Day 5 (Fig. 4D). Interestingly, glyphosate also inhibited the
270 formation of pigment that derives from auto-oxidation of L-DOPA (Fig. 4D). This implies that
271 glyphosate inhibited pigment production non-enzymatically.

272

273 **Phosphate-Containing Compounds Inhibited Melanization Similarly to Glyphosate**

274 To gain insight into the chemical features of glyphosate that inhibited melanogenesis we
275 assayed several structurally similar compounds using the same *in vitro* mushroom tyrosinase
276 assay. To test the effect of the amino acid functional group, we compared glyphosate alongside
277 its non-phosphate analog, glycine. We also tested the inhibitory effects of phosphoserine and
278 serine on melanin production. Phosphoserine inhibited dopaquinone, dopachrome, and melanin
279 formation to nearly the same extent as glyphosate (Fig. 5A-C). In contrast, neither glycine nor
280 serine inhibited dopaquinone, dopachrome, or overall melanin formation (Fig. 5A-C). We tested
281 the inhibitory effects of other phosphate-containing compounds including organophosphates
282 (phosphonoacetic acid), phosphoesters (pyrophosphate), and phosphoric acid. All of the
283 phosphate-containing compounds inhibited dopaquinone production (Fig. 5A) and dopachrome
284 formation (Fig. 5B) in a manner nearly identical to glyphosate, but differed slightly from each
285 other in melanin inhibition (Fig 5C).

286 Similar to glyphosate, these compounds all inhibited auto-oxidation of L-DOPA
287 comparably to their inhibition of tyrosinase-mediated melanin production (Fig. 5E). This further
288 illustrates that glyphosate and similar phosphate-containing compounds inhibit melanin in a non-
289 enzymatic fashion. These data suggest that the phosphate functional groups of these
290 compounds may be responsible for the melanin-inhibitory properties.

291

292 **Glyphosate Does Not React With L-DOPA or Inhibit Tyrosinase Directly**

293 We considered the possibility that glyphosate inhibited melanogenesis and dopaquinone
294 production by reacting with the L-DOPA substrate. To measure the reaction between these
295 compounds, we analyzed mixtures of L-DOPA and glyphosate by ¹H-NMR and ³¹P-NMR. We
296 found no evidence of interaction between the two compounds based on peak shifts of hydrogen

297 and phosphorous at both high (60 mM glyphosate and 20 mM L-DOPA) and low concentrations
298 (6 mM glyphosate and 5 mM L-DOPA) (Supplementary Fig. 4).

299 If glyphosate was inhibiting melanin production through the formation of a covalent bond
300 with tyrosinase, the inhibition should be irreversible. To test this, we treated 20 µg/ml tyrosinase
301 with 5.63 mg/ml (33.33 mM) glyphosate and removed the glyphosate by dialysis. The
302 glyphosate-treated enzyme had similar activity to the control (Fig. 6A), making a strong case
303 against a mechanism whereby glyphosate inhibited melanogenesis through irreversible
304 inhibition of tyrosinase. Instead, analysis of the tyrosinase reaction by Michaelis-Menten kinetics
305 assay with L-DOPA and glyphosate suggested that glyphosate is a non-competitive inhibitor of
306 melanin and dopachrome production (Fig. 6B). Further, we tested tyrosinase activity as a
307 function of enzyme concentration with and without glyphosate and constant concentration of L-
308 DOPA. We found that the slope of the glyphosate-treated enzyme is lower than the water-
309 treated control (Fig. 6C). This indicates that glyphosate-mediated inhibition is reversible (91,92).
310 Given that our findings showed that glyphosate inhibits auto-oxidation and tyrosinase-mediated
311 oxidation, we believe that the reversible inhibition is due to glyphosate interfering with the L-
312 DOPA substrate's ability *to be* oxidized rather than the enzyme's ability *to* oxidize. This could be
313 represented by the following where *E* represents tyrosinase, *S* represents L-DOPA, *I* represents
314 glyphosate, and *P* represents dopaquinone/melanin:

315 Normal Enzymatic Reaction: $E + S \rightleftharpoons ES \rightarrow P$

316 Inhibited Enzymatic Reaction: $E + S + I \rightleftharpoons E + SI \rightarrow P$

317 Copper ions are important for tyrosinase activity. Since glyphosate is a metal chelator
318 (93,94), we evaluated whether glyphosate's inhibitory effect was due to this property. We added
319 copper ions to the L-DOPA and tyrosinase reaction to rescue the glyphosate inhibition. We
320 performed the experiment with eight concentrations of copper (II) sulfate for each of the eight
321 glyphosate concentrations. In general, the addition of copper did not rescue the glyphosate
322 dependent inhibition of melanin (Fig. 6D). However, low concentrations of copper (6.25 - 25 µM)

323 increased tyrosinase activity, while high concentrations of copper (50 - 400 μ M) reduced activity,
324 indicating low copper can boost enzyme activity, while higher concentrations inhibit the reaction.
325 However, this hormesis-like effect was not observed at increasing glyphosate concentrations
326 (Supplementary Fig. 5). This result indicates that glyphosate's ability to chelate copper ions
327 could have a protective effect in high copper environments, which would otherwise lead to
328 negative effects on enzymatic activity and other biological processes. Similar results have been
329 previously seen in *Eisenia fetida* earthworms exposed to high copper conditions in soil (95).
330 Glyphosate contamination of copper-rich soil reduced the detrimental effects of the metal's
331 toxicity, presumably due to the glyphosate's copper chelation properties (95).

332

333 **Glyphosate Affects the Oxidative Properties of Melanogenesis**

334 Melanogenesis is dependent on the spontaneous radicalization of quinone intermediates
335 (96). Dopaquinone radicals and cyclodopa undergo a radical-mediated redox exchange that
336 converts cyclodopa into dopachrome and dopaquinone into L-DOPA. Further downstream, ROS
337 catalyze the polymerization of dihydroxyindole into eumelanin. Glyphosate's inhibitory effect
338 could be due to a role as a free-radical scavenger or antioxidant. Since the inhibitory
339 compounds blocked spontaneous oxidation of L-DOPA (Fig. 5E), they are antioxidants. To
340 measure this radical-quenching ability we used an ABTS assay in which ABTS radicals are
341 blue, but when quenched the solution becomes colorless. The degree of discoloration is a proxy
342 for radical concentration and antioxidant strength. Glyphosate quenched the ABTS radical to
343 some degree, but only after several hours of reaction (Supplementary Fig. 6A), which did not
344 occur with the other inhibitory phosphate-group containing compounds evaluated (Fig. 7A). This
345 indicates that direct free-radical scavenging may not be the primary mechanism of melanin
346 inhibition for glyphosate.

347 Phosphoric acid is a well-known synergist that boosts the antioxidant properties of
348 phenolic compounds. Phosphoric acid, and other synergists such as citric acid, malic acid, and

349 tartaric acid do not directly quench free radicals themselves, but instead work by regenerating
350 antioxidants, thus becoming “sacrificially oxidized”, or chelating metal ions in solution (97,98).
351 Alternatively, glyphosate could be reacting with existing antioxidants to strengthen and/or
352 regenerate them into “active” form. In this instance, the glyphosate would be bolstering the
353 antioxidant properties of L-DOPA.

354 We observed that the synergist citric acid inhibited melanization similarly to glyphosate
355 and phosphoric acid (Fig. 7B,C). The addition of glyphosate, phosphoserine, and phosphoric
356 acid enhanced the antioxidant properties of L-DOPA in an ABTS assay in a similar manner as
357 citric acid (Fig. 7D). This suggests that glyphosate may act as an inhibitor via antioxidant
358 synergism. The synergy is the ratio of the quenching capacity of the L-DOPA and the
359 compounds alone to the quenching capacity of L-DOPA combined with the compound. The
360 lower this ratio, the more synergistic the compounds are with L-DOPA (Supplementary Fig. 6B).
361 These values indicate that the inhibitory compounds are synergistic, whereas the non-inhibitory
362 glycine and serine are not as synergistic.

363 The inhibition of melanin was independent of the L-DOPA to glyphosate ratio, and
364 glyphosate’s IC_{50} is ~1 mM regardless of L-DOPA concentration (Supplementary Fig. 7). This
365 could be explained by a general antioxidant effect on solution.

366

367 **Glyphosate Alters the Oxidation-Reduction Potential of the System**

368 L-DOPA is a more effective antioxidant when it is oxidized or radicalized, and has a
369 better ability to form adducts with other radicals (99). Since glyphosate is acting as a synergistic
370 antioxidant, it may be driving L-DOPA oxidation and possibly radicalization in which L-DOPA
371 scavenges radicals better. This has the potential to disrupt melanin synthesis by stopping the
372 spontaneity of redox exchange and dopaquinone formation.

373 To investigate whether the addition of glyphosate changed the oxidation properties of L-
374 DOPA, we used cyclic voltammetry – a technique to measure the electrochemical properties of

375 solutions and previously used to study quinone electrochemistry (100,101). Voltammetry
376 performed on L-DOPA solutions with glyphosate showed dose-dependent shifts towards a
377 negative potential (Fig. 7E,H) in peaks that corresponded to L-DOPA oxidation (102) (**Peak 1**).
378 We validated these as L-DOPA oxidation peaks by performing voltammetry on various L-DOPA
379 concentrations (Supplementary Fig. 8A). The peak shift towards negative potentials indicates
380 the L-DOPA was oxidized more easily and had less ability to be an oxidant, similar to the
381 negative potential shifts associated with alkaline pH and increased oxidation (103). We
382 controlled for any pH-dependent peak shifts by adjusting each solution to pH 6.00 prior to
383 measurement. Decreased oxidizing power can lead to significant effects, as melanin
384 biosynthesis is reliant upon catechol oxidation and high redox potentials of quinones.
385 Interestingly, with increased glyphosate, the L-DOPA solution had a lower current intensity
386 associated with the reduction of dopaquinone to L-DOPA (**Peak 2**). In cyclic voltammetry,
387 smaller peaks indicate that less of the compound is oxidized or reduced. The decreased **Peak 2**
388 current became virtually non-existent with increasing glyphosate concentrations (Fig. 7E,H,I).
389 This implies that dopaquinone, represented by **Peak 2**, is either not being formed during L-
390 DOPA oxidation or cannot be reduced back into L-DOPA. These data indicate that the redox
391 cycling steps of melanization are halted due to the inability of dopaquinone to be reduced into L-
392 DOPA. This could also indicate that while L-DOPA was oxidized more in the presence of
393 glyphosate, it may form a non-dopaquinone product - either a radical-mediated dimer with itself
394 or a semiquinone.

395 396 **DISCUSSION**

397 We investigated the effect of glyphosate on melanin production in two species of insects,
398 *Galleria mellonella* and *Anopheles gambiae*, and found that both glyphosate and its major
399 metabolite AMPA were inhibitors of insect phenoloxidase and melanization. Although
400 glyphosate and AMPA are relatively weak inhibitors of these insects' melanization, the inhibitory

401 concentrations are relevant in the environment given the vast amounts used in agriculture, their
402 environmental stabilities, and the high potential for insect-herbicide interactions. Therefore,
403 glyphosate has a high potential to influence key insect physiological systems. We observed that
404 glyphosate enhanced the susceptibility to infection of two phylogenetically distinct insects, *G.*
405 *mellonella* and *A. gambiae*. This raises concerns and the suggestion that glyphosate may
406 interfere broadly with insect immunity through its effects on melanin-based defenses. Analysis
407 of *in vitro* tyrosinase and auto-oxidation models revealed that glyphosate inhibited melanization
408 by acting as a synergistic antioxidant and disrupting redox cycling. Overall, our findings provide
409 new insights on the complex reaction and suggest potential harmful effects of this herbicide on
410 non-target organisms, including some insects that may be important to ecosystem stability, and
411 already in peril due to the threat of an “insect apocalypse”.

412 *G. mellonella* treated with glyphosate were more susceptible to infection with *C.*
413 *neoformans*. Glyphosate treatment was associated with reduced size of melanized nodules in
414 the hemolymph following infection with *C. neoformans*. Two of three replicates showed
415 significantly reduced numbers of melanized nodules in the glyphosate-treated infections.
416 Nodules are primarily composed of hemocyte aggregates, released immune factors, and
417 melanin encapsulation of the pathogen, which function together to kill invading pathogens (22).
418 Altogether, these data suggest that glyphosate weakened the melanin-based immune response
419 of *G. mellonella*, which could have grave implications for host defense. *Galleria* are members of
420 the order Lepidoptera (moths and butterflies), which represent up 10% of known species on
421 Earth. Interactions with glyphosate in the soil, on plants during pollination, or ingested through
422 herbivory could contribute to immunocompromised lepidopteran populations. Glyphosate’s
423 effects on immunity in insects could compound a controversial and pre-existing problem of
424 declines in Lepidopteran biomass in recent decades (25,104–107).

425 Like our observations with *G. mellonella*, glyphosate made the *A. gambiae* mosquito
426 more susceptible to *P. falciparum* parasite infection, the primary agent of human malaria in

427 Africa. However, melanization is not considered the primary anti-*P. falciparum* immune
428 response in this malaria model (108). The increased susceptibility of *A. gambiae* to *P.*
429 *falciparum* could be due to broader alterations of mosquito immune defenses, or disruption of
430 non-melanin roles of catecholamine oxidation and phenoloxidase in insect immunity including
431 the production of ROS, cytotoxic intermediates, and pathogen lysis (3,13,109). Importantly, we
432 observed that even when infections of *A. gambiae* with *P. falciparum* resulted in an overall low
433 to no parasite burden in control-treated groups, glyphosate-treated groups exhibited a higher
434 infection burden and prevalence. This is notable because *Plasmodium* oocyte development
435 within the mosquito is a major bottleneck to successful vector competence in nature (110). If a
436 mosquito can prevent oocyst formation, there is no transmission of malaria to humans. The
437 numbers of oocysts from these low parasite burden experiments are in line with the normal
438 burden's found in natural field infection models (111,112). Our data may indicate that
439 mosquitoes exposed to glyphosate were less able to control *Plasmodium* infection they would
440 have otherwise resisted, thereby becoming potentially better vectors for malaria. Overall our
441 results raise concerns for public health and malaria control initiatives in regions in which malaria
442 is endemic and where there is increasing use of glyphosate, including areas of Latin America,
443 Sub-Saharan Africa, and Asia.

444 Our data revealed that uninfected adult female mosquitoes treated with glyphosate
445 displayed a hormesis-like dose-dependent effect when measuring survival outcomes. Survival
446 increased at low doses of glyphosate compared to the control. This greater longevity may be
447 due in part to reduced basal damage from host defense mechanisms that normally occur during
448 melanin formation, and/or altered gut microbiota. In contrast, mosquitoes exposed to high
449 concentrations of glyphosate showed decreased survival. These data suggest the broader
450 notion that glyphosate could have varied and complex outcomes on vector competence
451 depending on its concentration in the environment. The low-concentration glyphosate
452 treatments resulted in longer-lived, yet immunosuppressed, mosquitoes that were slightly more

453 susceptible to infection with *P. falciparum*, whereas short-lived high glyphosate treated
454 mosquitoes were much more susceptible to *P. falciparum*. Further, while the 10 mM-treated
455 mosquitoes had the worst survival outcome, the mosquitoes that survived the drugging showed
456 low susceptibility to *P. falciparum* infection. These observations suggest a potentially interesting
457 effect whereby very high concentrations of glyphosate reduce mosquito survival, but bolster the
458 immune system or general physiology of survivors, which then allows them to resist *P.*
459 *falciparum* infection with greater success. Alternatively, very high glyphosate treatment could be
460 selecting for mosquitoes within the population more resistant to *P. falciparum* infection.

461 Our analyses of *A. gambiae* midgut microbiota indicated that glyphosate did not impact
462 *A. gambiae* midgut culturable bacterial density; although the herbicide did perturb midgut
463 microbiota composition in a non-dose dependent manner. More specifically, glyphosate altered
464 diversity of the microbial community, and glyphosate-treated mosquitoes exhibited diminished
465 Enterobacteriaceae and expanded *Asaia spp.* populations. The presence of some
466 Enterobacteriaceae, including the common insectary contaminant *Serratia marcescens*, in
467 *Anopheles spp.* midguts is associated with lower susceptibility to *Plasmodium spp.* infection
468 (113,114). This effect is observed quantitatively by the significantly different prevalence of
469 individual bacterial taxons (beta diversity) between the glyphosate and control-treated
470 microbiota, while there is an overall unchanged number of bacterial taxa present (alpha
471 diversity). Beta diversity analysis indicates that microbial communities associated with
472 glyphosate-treated mosquitoes cluster together and are different than those from control
473 mosquito communities.

474 Our results are consistent with reports that glyphosate perturbs the microbiota of
475 honeybees that makes them more susceptible to infection (59). Our data suggests that while
476 glyphosate may perturb the microbiota and affect immunity as previously described (59,60), it
477 can also inhibit melanization which is a critical part of insect immune defense. We do not see a

478 dose-dependent effect of glyphosate on the microbiota composition, but we do see a dose-
479 dependent effect on mosquito susceptibility to *Plasmodium* infection; this indicates that the
480 enhanced susceptibility might be unrelated to microbiome perturbations. These mechanisms of
481 susceptibility are not mutually exclusive and could be additive to weaken insect health.
482 Additionally, while AMPA does not to disrupt the microbiota of honeybees (60), we show it can
483 inhibit melanization of *G. mellonella* phenoloxidase and mushroom tyrosinase. A recent study in
484 *Apis cerana cerana* honeybees indicate that glyphosate-based herbicide treatment increases
485 expression of wound and defense genes, including those related to melanization (115).
486 Interestingly, this study also showed that glyphosate feeding decreased the expression of many
487 odorant binding proteins, which have been shown to mediate the melanization response in both
488 Tsetse fly (*Glossina morsitans morsitans*) and *Drosophila melanogaster* (116) This suggests
489 complex regulation of melanization following treatment with glyphosate-based herbicide,
490 including the possibility of increased melanin-related gene expression as a compensation for
491 glyphosate's inhibitory effects. Additionally, other surfactants and components of the
492 commercial herbicide formulation used could trigger damage and immune gene expression.

493 Melanins and phenoloxidases are involved in other physiological functions in insects
494 including proper pupation, and cuticle and eggshell development. In our experiments, which
495 involved single dosing or short duration of feeding, we did not detect a difference in coloration of
496 adult mosquito treated with glyphosate, nor a defect in *G. mellonella* pupation following
497 glyphosate treatments of final instar larvae. However, we cannot rule out that longer glyphosate
498 exposure or feeding throughout the lifecycle would effect these functions. If such effects
499 happen, they will only compound the effects of glyphosate on melanin-based immunity and
500 insect physiology.

501 We sought to understand the mechanism of melanization inhibition by glyphosate. The
502 process of melanization is highly dependent upon oxidation and redox cycling between
503 catechols and quinones. The melanin production process is halted if the oxidizing ability and the

504 redox potentials are altered. Melanization begins with the conversion of L-DOPA into
505 dopaquinone through enzymatic or spontaneous oxidation of L-DOPA, followed by redox cycling
506 that results in dopachrome formation, and subsequently melanin polymerization. Glyphosate
507 inhibited formation of dopaquinone and melanin pigment mediated by both tyrosinase and auto-
508 oxidation, which strongly suggests that glyphosate inhibits L-DOPA oxidation in an enzyme
509 independent manner. We found that other phosphate-containing compounds inhibited
510 melanization in a similar manner including phosphoserine, phosphoacetic acid, pyrophosphate
511 and phosphoric acid. This is in line with literature reports that other aminophosphonic acids
512 inhibit fungal eumelanin in the human pathogen *Aspergillus flavus* (117). Incidentally, this class
513 of compounds is patented for use in human cosmetics, and are marketed as solutions to inhibit
514 melanogenesis in the skin (118,119).

515 We found no evidence that glyphosate irreversibly inhibited tyrosinase activity or directly
516 interfered with enzyme function. Addition of copper ions did not rescue the inhibition, indicating
517 that the copper-based catalytic core of tyrosinase is not disrupted by glyphosate. Interestingly,
518 low copper increased tyrosinase activity and high doses reduced activity. However, copper had
519 minimal effects on tyrosinase activity during high glyphosate concentrations. It appears that
520 glyphosate, possibly through chelation, acts as a “buffer” of copper ions and can reduce the
521 metal’s harmful effects, similar to previous findings concerning the toxicity of high-copper soil to
522 earthworms following glyphosate treatment (95). This could have broader implications for
523 melanogenesis in nature, where some fungi use copper as a signal to upregulate melanin-
524 producing enzymes (120), and thus copper ion sequestration could reduce melanin production.

525 We examined the ability of glyphosate and the other compounds to quench free radicals,
526 which are necessary to the melanization process. Of the inhibitors tested, only glyphosate had
527 radical-quenching activity, but this occurred relatively slowly compared to the typical timeframe
528 of antioxidant reactions reported in literature (121). This property is likely not the mechanism of
529 inhibition as phosphoserine has a similar structure and near identical inhibition of melanization

530 as glyphosate, yet no radical-quenching properties. While not a free-radical quencher,
531 phosphoric acid is a known antioxidant synergist – a class of compounds that enhance
532 antioxidant properties of phenolic compounds by chelating metals or reverting antioxidants into
533 their active states (98). Synergists like phosphoric acid, citric acid, malic acid, and alpha-
534 hydroxy acids are added to foods, medicines, and cosmetics at concentrations up to 10% as a
535 preservative due to their synergist effects on antioxidants (122). Glyphosate behaved similarly
536 to phosphoric acid and citric acid; citric acid inhibited melanization similarly to glyphosate and
537 phosphoric acid, suggesting an inhibition mechanism via antioxidant synergy. Additionally, we
538 report that glyphosate and other inhibitors have synergistic effects on the antioxidant properties
539 of L-DOPA. L-DOPA's antioxidant properties derive from its reduction back to a normal state
540 from an oxidized state, or a radical-mediated adduction reaction with the oxidized compounds in
541 solution. Since glyphosate makes L-DOPA a more efficient antioxidant, glyphosate thus alters
542 the oxidative balance of L-DOPA and/or produces a buildup of radical or semiquinone
543 intermediates.

544 Consistent with these findings of antioxidant synergy, cyclic voltammetry revealed that
545 glyphosate decreased the L-DOPA-Dopaquinone redox potential. Hence, L-DOPA becomes
546 both a weaker oxidizing agent and a stronger reducing agent (antioxidant) and is more prone to
547 oxidation in the presence of the herbicide. Glyphosate decreased dopaquinone reduction in a
548 dose dependent fashion indicating that dopaquinone cannot be reduced or is not produced
549 following L-DOPA oxidation. A lack of dopaquinone could indicate that glyphosate causes
550 oxidized L-DOPA semiquinone intermediates to remain stable or react with each other and form
551 L-DOPA dimers. On the other hand, if dopaquinone cannot be reduced into L-DOPA,
552 melanization becomes unfavorable as redox exchange could not occur. These changes in
553 voltammogram do not appear when the L-DOPA solution is treated with 16 mM glycine, but did
554 occur with citric acid. This further supports that glyphosate is acting as a synergistic antioxidant
555 and prevents the redox-dependent melanization.

556 Our findings investigating glyphosate's mechanism of melanin inhibition points to
557 disruption of oxidative balance and redox cycling which may result in the buildup of toxic
558 oxidative intermediates. Previous studies evaluating glyphosate's impact on organisms show
559 that the herbicide increases oxidative stress, lipid peroxidation, and antioxidant responses in
560 bacteria, plants, arthropods, fish, amphibians, rats, and human red blood cells (69–76). These
561 data bolster our findings that glyphosate promotes oxidation in phenolic compounds like L-
562 DOPA and inhibits clearance of oxidative stress. Understanding the mechanisms by which
563 compounds such as glyphosate might impact insect biomass and contribute to a potential insect
564 decline is important, as they have both direct and indirect impacts on human health.

565 Glyphosate's interference with melanization could have considerable environmental
566 impact given its stability and wide concentration range, from over 50 mM at time and at site of
567 application to under 1 nM in runoffs from application sites (33,39,123). At higher
568 concentrations, glyphosate could inhibit melanin production in some insects, thus rendering
569 them more susceptible to pathogens due to reduced immune competence. This suggests
570 protean consequences for human health ranging from ecosystem disruption to altered vector
571 competency of lethal human pathogens and increased malaria transmission in endemic regions
572 that use glyphosate-based herbicides in agriculture. Importantly, we provide evidence that
573 glyphosate enhances *A. gambiae* susceptibility to the human malaria parasite, which could
574 potentially make it a better vector for transmitting disease to humans. Our data in *Galleria* and
575 *Anopheles* can perhaps be extrapolated to other lepidopteran (moth and butterfly) and dipteran
576 (fly) species with additional importance to the environment.

577 In summary, our results suggest that glyphosate interferes with melanization in two
578 insect species, through a mechanism involving altering the redox potential of melanin
579 polymerization reaction. This phenomenon is concerning because of the importance of
580 melanization in insect immunity. A strong immune response is vital for insect survival, and
581 disruption of their immune function, including the inhibition of melanization, could be disastrous

582 for these animals. Insects are pivotal members of the world's ecosystems, essential to
583 maintaining proper function, and they ensure human food security. Yet, certain data indicates a
584 drop in insect biomass over recent decades, a phenomenon that has been called the "insect
585 apocalypse" (25,104,105,124,125). Although this view has been questioned regarding the true
586 extent and possible causes of the insect population declines (126–130), our results suggest that
587 glyphosate use as a mechanism by which insect immunity can be undermined by human
588 activities.

589

590 **ACKNOWLEDGEMENTS**

591 We would like to acknowledge Dr. Gene Fridman in the Johns Hopkins School of
592 Medicine for lending the use of the Fridman lab's Metrohm Autolab potentiostat for use in the
593 cyclic voltammetry experiments. We would like to thank the Johns Hopkins Malaria Research
594 Institute and the Department of Molecular Microbiology and Immunology Insectary and Parasite
595 Core facility, and Dr. Joel Tang from the Johns Hopkins NMR Core facility for his help with the
596 NMR experiments. We would also like to thank the entire Casadevall Lab for their suggestions
597 and inputs during conversations and their feedback during lab meetings and presentations.
598 Figures in Supplementary Figure 9 were made using BioRender. DFQS, EC, and AC are funded
599 by the Johns Hopkins Malaria Research Institute Pilot Grant Casadevall_123; DFQS, EC, and
600 AC are funded by NIAID R01 AI052733; DFQS has been funded by NIH grants
601 5T32GM008752-18 and 1T32AI138953-01A1; AJB and NAB are funded by NIH grant National
602 Institutes of Health R35GM128871.

603

604 **AUTHOR CONTRIBUTIONS**

605 D.F.Q.S. contributed to conceptualization, methodology, formal analysis, investigation, data
606 curation, writing of the original draft and subsequent editing, data visualization, and project
607 administration. E.C. contributed to conceptualization, methodology, investigation, resources,

608 reviewing and editing of manuscript, supervision, project administration, and funding acquisition.
609 R.T. contributed to conceptualization, methodology, resources, reviewing and editing of
610 manuscript, and supervision. A.J.B. contributed to conceptualization, methodology, software
611 use, formal analysis, investigation, data curation, reviewing and editing of manuscript,
612 visualization, and project administration. Y.D. contributed to methodology and reviewing and
613 editing of manuscript. G.D contributed to reviewing and editing of manuscript, resources, and
614 funding acquisition. N.A.B. contributed to conceptualization, methodology, investigation,
615 resources, reviewing and editing of manuscript, supervision, project administration, and funding
616 acquisition. A.C. contributed to conceptualization, methodology, resources, supervision, project
617 administration, and funding acquisition.

618

619 **DECLARATION OF COMPETING INTERESTS**

620 The authors declare no competing interests.

621

622 **METHODS**

623 **Biological materials**

624 *Galleria mellonella* larvae were obtained through Vanderhorst Wholesale Inc, St. Marys,
625 Ohio, USA. *Cryptococcus neoformans* strain H99 (serotype A) was kept frozen in 20% glycerol
626 stocks and subcultured into Sabouraud dextrose broth for 48 h at 30°C prior to each
627 experiment. The yeast cells were washed twice with PBS, counted using a hemocytometer
628 (Corning, Inc), and adjusted to 10⁶ cells/ml.

629 *Anopheles gambiae* (Keele strain) mosquitoes were maintained on sugar solution at
630 27°C and 70% humidity with a 12 h light to dark cycle according to standard rearing condition.

631 *Plasmodium falciparum* NF54 (Walter Reed National Military Medical Center, Bethesda)
632 infectious gametocyte cultures were provided by the Johns Hopkins Malaria Research Institute
633 Parasite Core Facility and were diluted to 0.05% gametocytemia with naïve human blood before

634 feeding to the mosquitoes using an artificial glass membrane feeder as established in (Dong et
635 al., 2009) (83).

636 **Compound and Dilution Preparation**

637 Each compound, including the glyphosate (Millipore Sigma, Product #45521), was
638 prepared in 300 mM stock solution in Milli-water Q and brought to a pH of 5.5, and 20 µl of each
639 compound was serially diluted 1:2 in PBS (pH 7.4), with a compound-free control. When all
640 reaction components are added, the final concentrations of the compounds in these dilutions
641 were 33.33, 16.67, 8.33, 4.17, 2.08, 1.04, 0.52, and 0 mM.

642 ***Galleria mellonella* Hemolymph Extraction and Phenol Oxidase activity**

643 Healthy (active and cream-colored) larvae were cold anesthetized, punctured in their
644 proleg with 18G needle and pressure was applied to the larvae to promote bleeding of
645 hemolymph. Hemolymph was collected from larvae directly into an eppendorf tube.
646 Anticoagulants were not used as they might interfere with the melanization process.

647 For automelanization experiments, hemolymph was diluted 1:10 in PBS and mixed with
648 a pipette. Then, 160 µl of 1:10 hemolymph is added to 20 µl of glyphosate serially diluted in
649 PBS. The change in absorbance at 490 nm was recorded and analyzed as described above.

650 For experiments with L-DOPA, hemolymph was diluted 1:5 in PBS and mixed by pipette.
651 Experiments were performed as per the phenoloxidase activity assay in (Cornet, Gandon, and
652 Rivera, 2013 (131)).

653 To test the effect of glyphosate on hemocytes viability, hemolymph was diluted 1:2 with
654 anticoagulation buffer (132), as melanization was not of importance for this experiment.
655 Hemocytes were pelleted and suspended in anticoagulation buffer. Glyphosate was added to an
656 aliquot of hemocytes in solution and incubated with mixing on a rocker at 30°C for 15 min.
657 Hemocyte viability was assessed by 0.02% trypan blue staining and enumeration of stained
658 (dead) versus unstained (alive) hemocytes with a hemocytometer.

659 ***Galleria mellonella* Infection and Survival**

660 Healthy final instar *G. mellonella* larvae weighing between 175 and 225 mg were
661 selected, and left starving overnight. Groups of larvae were injected with 10 μ l of PBS or 10 μ l of
662 1 mM sterile glyphosate in PBS. Larvae were monitored and left to recover for 5 h. Larvae were
663 then injected with 10 μ l of sterile PBS or injected with 10^4 *Cryptococcus neoformans* yeast cells
664 per larva. Due to the low concentration of glyphosate administered to the larvae, their volume of
665 hemolymph, and their body volume, we believe the approximate concentration of glyphosate is
666 below the concentrations required to inhibit *C. neoformans* growth (26). *G. mellonella* larvae and
667 pupae were kept at 30°C and monitored daily for survival for 14 d. Survival was assessed by
668 movement upon stimulus with a pipette. See Supplementary Fig. 9a.

669 **Melanization and Nodule Measurements**

670 *G. mellonella* larvae were drugged and infected as described above in groups of 3 larvae
671 per condition. After 24 h, larval hemolymph was removed directly in anticoagulation buffer,
672 centrifuged at 10,000 xg for 5 min, and resuspended in coagulation buffer.

673 Brightfield microscopy images were randomly taken at 4x magnification, with 15-20
674 images taken per condition per replicate. These images were analyzed using Fiji (133) Particle
675 Analyzer function using with a threshold set between 0 and 120 mean gray value. Particle area
676 and numbers were calculated. Additional images were taken of nodules at 20x and 100x
677 magnification, the latter of which were used to manually score the degree of melanization of
678 fungal cells within the nodules. Statistical significance of differences between melanized particle
679 area was analyzed using a nested non-parametric Mann-Whitney-Wilcoxon rank test using the
680 *nestedRanksTest* package (*Version 0.2*, D.G. Scofield, 2014)(134) in R for R 4.0.2 GUI 1.72 for
681 Mac OS at <https://www.r-project.org/> (R Core Team, 2020).

682 ***Anopheles gambiae* Phenol oxidase activity**

683 Phenoloxidase activity assays were performed as previously described (135).
684 Experiments were done in biological triplicate with different batches of mosquitoes, as well as in
685 technical triplicate per biological replicate of 3 batches of 10 mosquitoes.

686 ***Anopheles gambiae* Survival**

687 Adult female mosquitoes of *A. gambiae* Keele strain were raised on 10% sucrose for
688 three days post-emergence. On the third day, adult females were sorted into seven groups of 40
689 and placed into mesh-covered cardboard cups and provided a cotton ball with 10% sucrose
690 mixture with either 0 μ M (Control), 30 μ M, 100 μ M, 300 μ M, 1 mM, 3 mM, or 10 mM glyphosate.
691 The cotton balls were replaced every third day with new cotton balls and fresh
692 sucrose/glyphosate solutions. Mosquito death was monitored daily for 14 days. Experiments
693 were performed in three independent replicates, for a total of 120 mosquitoes in each treatment
694 group.

695 ***Anopheles gambiae* Cuticle Pigmentation and Wing Size**

696 Adult female mosquitoes were drugged for 5 days as previously described. Mosquitoes
697 were cold euthanized and mounted dorsally on a slide with double-sided tape. Images of the
698 mosquito ventral abdomen were taken under a dissection microscope with constant exposure
699 and lighting conditions. Pigmentation was measured using Fiji software (133). The entire
700 abdomen of each mosquito was selected using a freehand selection tool, and the 8-bit mean
701 gray value was measured using the Measure tool. A measurement of 0 corresponds to a pure
702 black gray value, whereas 255 corresponds to a pure white gray value.

703 Following abdomen pigmentation measurements, mosquito bodies were removed, with
704 careful attention to keeping the wings remaining intact on the tape. Intact wings were imaged on
705 a microscope, and the length of the individual wing lengths were measured from tip-to-tip using
706 Fiji Measure tool.

707 ***Anopheles gambiae* infection with *Plasmodium falciparum***

708 Adult female mosquitoes (3-4 d old) of *A. gambiae* Keele strain were sorted and drugged
709 as described above. On the fifth day of glyphosate exposure, mosquitoes were provided a blood
710 meal containing *P. falciparum*. Blood-fed engorged mosquitoes were sorted on ice and fed 10%
711 sucrose *ad libitum* for 8 d. Midguts were dissected and stained with 0.2% Mercurochrome

712 solution and oocysts were enumerated using a 20X objective with light microscopy. See
713 Supplementary Fig. 9b.

714 ***Anopheles gambiae* Midgut Microbiome Analysis**

715 Adult female mosquitoes (3-4 d old) of *A. gambiae* Keele strain were sorted and drugged
716 as described above. On the fifth day of glyphosate exposure, mosquitoes were sterilized in
717 ethanol for 2 minutes, washed, and dissected in sterile PBS. The midguts were removed, placed
718 in 500 µl sterile PBS on ice, homogenized, diluted, and plated on LB agar plates. Plates were
719 incubated at 30°C for three days and individual colonies were counted. Each experiment used
720 10-20 mosquitoes per condition, and the experiment was performed three independent times.

721 For the 16S rRNA sequencing studies, mosquitoes were reared, drugged, and then
722 midguts were dissected as described above, with five individual midguts per condition. DNA was
723 extracted from frozen mosquito samples using the Lucigen EpiCentre MasterPure DNA
724 extraction kit. The bacterial 16S rRNA gene was amplified by PCR, and sample-specific Illumina
725 adapters were ligated to the PCR products. PCR products from multiple samples were pooled
726 and sequenced on the Illumina MiSeq platform by the University of Connecticut MARS Facility.
727 Data were then analyzed using mothur (136) to construct contigs to align forward and reverse
728 reads, remove ambiguous bases and chimeric regions, align sequences to the Silva 16S V4
729 reference database, and cluster reads into 3% operational taxonomic units (OTUs). Sequences
730 derived from known contaminants were selectively removed. Alpha and beta diversity
731 measurements were performed using the Shannon diversity index and Bray-Curtis dissimilarity
732 distance respectively. Bray-Curtis distances were graphed on principal coordinates analysis
733 (PCoA) plots in two dimensions. Taxa and PCoA graphs were produced using
734 MicrobiomeAnalyst (137,138). See Supplementary Fig. 9c.

735 **Dopaquinone Formation MBTH Assay**

736 Quinones like dopaquinone are unstable and difficult to study directly; thus,
737 dopaquinone quantification relies on the formation of a stable adduct with MBTH (3-methyl-2-

738 benxothioxolinone hydrazine) that forms a pigment that absorbs at 505 nm(139). This
739 absorption overlaps with the absorption of another melanin intermediate, dopachrome (Q), but is
740 not expected to interfere since dopaquinone reaction with MBTH prevents dopachrome
741 formation. Further, the molar absorbance coefficient for MBTH-Dopaquinone is more than 10
742 times higher (39,000 L/[mol cm]) than that of dopachrome (3,700 L/[mol cm]), and interference
743 from dopachrome would be relatively small.

744 MBTH reaction mixtures were prepared as previously described (139). This mixture is
745 warmed at 42°C to help solubilize the components. Then, 5 µl of 2 µg/ml Mushroom Tyrosinase
746 (Sigma, Product #T382) and 20 µl of 20 mM L-DOPA are added to the MBTH solution, and 160
747 µl of the solution is immediately added to each well containing compounds. The plate was read
748 at an absorbance of 505 nm for 30 min at 30°C, and read again at 1 h and overnight. The
749 dopaquinone levels are determined by the formation of the bright pink adduct between the
750 quinone and the MBTH.

751 **Dopachrome and Melanin Measurements**

752 Tyrosinase activity was determined as previously described (135), substituting
753 mushroom tyrosinase for phenoloxidase. The formation rate of dopachrome is measured as the
754 maximum velocity of this reaction, and the dopachrome levels are measured as the absorbance
755 at 490 nm after 30 min as the absorbance values plateau. Melanin levels are measured as the
756 absorbance at 490 nm after the reaction has continued for 5 d in the dark at room temperature.

757 **Free-Radical Scavenging ABTS Assay**

758 ABTS solution was prepared as previously described (140). To test the radical-
759 scavenging capability of the compounds, 10 µl of the compounds were serially diluted in a 96
760 well plate as previously described, and 90 µl of diluted ABTS was added to each well. The 734
761 nm absorbance was measured immediately, after 10 min, 1 and 2 h. In kinetics experiments,
762 absorbance readings were taken every two minutes for 5 h.

763 To measure the radical scavenging capacity of the synergistic compounds and L-DOPA
764 mixtures, ABTS was prepared and diluted in Milli-Q water. In each well, 5 μ l of compound stocks
765 were added with either 5 μ l of water or 5 μ l of 500 μ M L-DOPA. Next, 90 μ l of ABTS solution
766 was added to the well, and the absorbance was read immediately at 734 nm. Synergy was
767 calculated from this data using the following formula:

$$768 \quad \text{Synergy Ratio} = \frac{(\Delta\text{Abs } 734 \text{ Compound Alone} + \Delta\text{Abs } 734 \text{ DOPA Alone})}{\Delta\text{Abs } 734 \text{ Compound with DOPA}}$$

769 **Glyphosate Effect on L-DOPA**

770 To determine if L-DOPA is reacting with glyphosate, we analyzed by NMR. We diluted
771 300 mM stock of glyphosate in water to 60 mM (10 mg/ml) in D₂O, prepared 20 mM (4 mg/ml) L-
772 DOPA in D₂O, and prepared two mixtures of glyphosate and L-DOPA: one with 20 mM (4
773 mg/ml) L-DOPA and 60 mM (10 mg/ml) of glyphosate in D₂O, and another with a low
774 concentration of 1 mg/ml for both compounds equaling 5 mM L-DOPA and 6 mM glyphosate.
775 We then performed ³¹P-NMR and ¹H-NMR on these samples.

776 **Glyphosate Effect on Tyrosinase**

777 To determine the tyrosinase kinetics with glyphosate as an inhibitor, we serially diluted
778 155 μ l of 20 mM L-DOPA in Milli-Q water. To each dilution of L-DOPA we added 20 μ l of
779 glyphosate diluted in PBS and 5 μ l of 2 μ g/ml mushroom tyrosinase to the reaction mix. In order
780 to account for non-enzymatic oxidation of L-DOPA, we ran an experiment in parallel, in which
781 we added 5 μ l of Milli-Q water instead of tyrosinase. The reaction mix was kept at 30°C for 24 h.
782 The plate was read at 490 nm. To calculate enzyme-specific oxidation of L-DOPA, the no
783 enzyme values were subtracted from the tyrosinase rows. The kinetics curve is plotted as a
784 function of absorbance after 24 h of reaction time versus concentration of L-DOPA.

785 We tested if tyrosinase concentration had an effect on the percent inhibition of the
786 reaction. We prepared dilutions of tyrosinase. We added 5 μ l of each dilution to a 96-well plate,
787 and added 135 μ l of Milli-Q water, 20 μ l of 20 mM L-DOPA, and 20 μ l of glyphosate in PBS. We

788 measured maximum velocity of this reaction at 490 nm. The difference in velocities and percent
789 inhibition reported were calculated by difference = $V_{\max \text{ water}} - V_{\max \text{ glyph}}$, and percent inhibition =
790 $100 \cdot (V_{\max \text{ glyph}} / V_{\max \text{ water}})$.

791 To determine if glyphosate irreversibly affects tyrosinase activity, 450 μL of 20 $\mu\text{g}/\text{mL}$
792 mushroom tyrosinase was prepared in 450 μL of 50 mM sodium phosphate buffer, pH 7, either
793 with 50 μL of 300 mM glyphosate, or 50 μL of Milli-Q water. The enzyme solution was loaded into
794 a hydrated 10,000 MWCO Slide-a-lyzer dialysis cassette (Thermo Scientific), and the enzyme
795 solutions were dialyzed in a 50 mM sodium phosphate buffer at 4°C, according to the
796 manufacturer's protocol. Protein concentrations were measured and normalized using sodium
797 phosphate buffer. To measure the kinetics of the control enzyme versus the treated enzyme, a
798 kinetics assay was performed as previously described. Each reaction's maximum velocity is
799 determined and plotted.

800 **Copper Rescue of Melanin Inhibition**

801 As previously described, serial dilutions of glyphosate were arrayed in eight rows; one
802 row per copper ion concentrations to be tested. Copper sulfate was prepared and serially diluted
803 and 10 μL of the copper solution is added to each well containing the glyphosate dilution. To
804 each well 150 μL of reaction mix (125 μL of Milli-Q water, 20 μL of 20 mM L-DOPA, and 5 μL of
805 2 $\mu\text{g}/\text{mL}$ mushroom tyrosinase (5 μL of water used for auto-oxidation experiments) was added.
806 The final copper ion concentrations were 400, 200, 100, 50, 25, 12.5, 6.25, and 0 μM . The
807 dopachrome and melanin measurements are reported as previously described.

808 **Cyclic Voltammetry**

809 Cyclic voltammetry was performed using a Metrohm Autolab potentiostat (Switzerland),
810 3 mm Glassy Carbon working electrode, 10 mm x 10 mm x 0.1 mm platinum plate counter
811 electrode, and an Ag/AgCl reference electrode in 3 M KCl solution. Solutions were prepared in
812 0.1x PBS (Difco) at a pH 6.00, adjusted with NaOH and HCl. 10 mL of L-DOPA solution was
813 freshly prepared in this buffer, and 1 mL of glyphosate, glycine, water, etc, solution at pH 6.00

814 were added to the L-DOPA. Readings were done with three tracings at a scan rate of 50 mV/s
815 at intervals of 5 mV steps. Glassy carbon electrode was washed and polished between readings
816 with slurry of alumina powder and water on cloth pads.

817

818 DATA AVAILABILITY

819 The 16S rRNA sequencing datasets generated during this study are available at Mendeley Data
820 at DOI:10.17632/6ymh76hmzm.1, and the datasets from the remaining experiments are
821 available at Mendeley Data at DOI: 10.17632/xndcmbn6wd.2.

822

823 FIGURE LEGENDS

824 **Fig. 1. Glyphosate Inhibits *G. mellonella* Melanization and Increases Infection**

825 **Susceptibility. (A)** Glyphosate inhibits the phenoloxidase activity of 1:10 dilutions of
826 hemolymph without exogenously added L-DOPA. **(B)** AMPA, a primary metabolite of
827 glyphosate, inhibits *G. mellonella* phenoloxidase-mediated melanization similar to glyphosate.
828 Error bars in **(A-B)** represent \pm SD **(C)** *G. mellonella* larvae drugged with glyphosate solution
829 (10 μ l of 1 mM) in PBS and infected 5 h post treatment with 10^4 cells of WT *C. neoformans* die
830 rapidly compared to PBS-treated controls. Death events were recorded daily. Each infection
831 condition represents survival of 95 animals, pooled together from four biological replicates, and
832 six total technical replicates. Statistical significance was assessed by Gehan-Breslow-Wilcoxon
833 test, which we used to place weight on early timepoints in the survival curve. We used this test
834 because we expected to see the glyphosate-mediated differences early in the infection due to
835 the timing of the glyphosate treatment. Since we where the expected effects of the one-time pre-
836 treatment with glyphosate would be. **(D)** The size of the dark melanized particles within nodules
837 upon *C. neoformans* infection are significantly smaller in the glyphosate-treated (10 μ l of 1 mM)
838 infected groups compared to the PBS-treated infected groups, which were analyzed for
839 significance using a nested non-parametric Mann-Whitney-Wilcoxon rank test. Horizontal bar

840 represents the median value and the error bars represent the 95% Confidence Interval **(E)** The
841 degree of melanin encapsulation of the yeast within the nodule is also reduced in the
842 glyphosate-treated (10 µl of 1 mM) groups, as measured on a scale of 0 (no melanin
843 encapsulation) to 4 (very high levels of melanin encapsulation) as demonstrated in **(F)**.
844 Numbers in each bar represent the number of encapsulated *C. neoformans* for each score.
845 Statistical significance was assessed using a Chi-squared table test. Data in **(D)** and **(E)**
846 represent data over three independent replicates with three larvae used per condition per
847 replicate. **(G)** Representative brightfield micrographs showing the hemocyte and nodule
848 formation in the different treatment groups at 20x and 100x magnification. Scale bars represent
849 10 µm. Nested non-parametric Mann-Whitney-Wilcoxon rank test performed using R for R 4.0.2
850 GUI 1.72 for Mac OS at <https://www.r-project.org/> (R Core Team, 2020) and the *nestedRanksTest*
851 package (*Version 0.2*, D.G. Scofield , 2014)(134). All other statistical analyses performed using
852 GraphPad Prism version 8.4.3 for Mac OS, GraphPad Software, San Diego California USA,
853 www.graphpad.com. See also, Supplementary Fig. 1.

854

855 **Fig. 2. Glyphosate Effects on *A. gambiae* Phenoloxidase Activity and Susceptibility to**
856 ***Plasmodium* Infection.** **(A)** Glyphosate inhibits phenoloxidase activity in *A. gambiae* homogenate.
857 Enzyme activity represents three biological replicates with three technical replicates for each
858 condition. **(B)** Glyphosate treatment increases the susceptibility of the *A. gambiae* to *P. falciparum*
859 infection as measured by oocyst count per midgut. Increased glyphosate doses are associated with
860 increased median oocyst burden. Parasite infection represents four biological replicates and four
861 separate infections, line indicates median, and differences in parasite burden analyzed for
862 significance using non-parametric Kruskal–Wallis test with each group compared to the control
863 group with Dunn’s correction for multiple comparisons. **(C)** Low doses of glyphosate enhance the
864 survival of adult mosquitoes, while the higher doses diminish their survival as compared to the
865 control. Survival curves represent 120 animals from three independent replicates composed of

866 groups of 40 mosquitoes, and survival was examined for statistical significance using the Log-Rank
867 Mantel-Cox analysis with a Bonferoni correction for multiple comparisons. (D) Hazard ratios
868 calculated from the Cox Mixed Effects Model to account for fixed (glyphosate treatment) and
869 random effects (replicate). Hazard ratios <1 indicate lower risk of death compared to control values,
870 and values >1 indicate a higher risk of death compared to the control. Hazard Ratio of 1 is depicted
871 by a dotted line. The Cox Mixed Effects modeling was performed using R for R 4.0.2 GUI 1.72 for
872 Mac OS at <https://www.r-project.org/> (R Core Team, 2020) and the *coxme* package (Version 2.2-16,
873 T.M. Therneau, 2020)(141). All other statistical analyses performed using GraphPad Prism
874 version 8.4.3 for Mac OS, GraphPad Software, San Diego California USA, www.graphpad.com.
875 The statistical significance in (C) is coded as: ns - $p > 0.05$, * - $p < 0.05$, ** - $p < 0.01$, *** - $p < 0.001$,
876 and **** - $p < 0.0001$. See also Supplementary Fig. 2.

877

878 **Fig. 3. Glyphosate Alters the Composition, but Not Density, of the *A. gambiae* Midgut**

879 **Microbiota.** (A) Glyphosate does not alter microbial density of the culturable mosquito midgut
880 bacteria (grown on LB agar). Each sample consists of 40-50 individual mosquito midguts over three
881 independent replicates. Error bars represent the mean and \pm SD. (B) Glyphosate alters the
882 composition of the mosquito microbiota, leading to decrease of Entereobacteriaceae and an increase
883 of *Asaia* spp. (C) The glyphosate treatments do not significantly alter alpha diversity as measured by
884 the Shannon Index (statistical analysis conducted using one-way ANOVA; NS = $p > 0.05$). (D)
885 However, the glyphosate-treated and control-treated microbiota form distinct clusters in principle
886 coordinates analysis, measured by Bray-Curtis dissimilarity. Statistical significance was tested by
887 PERMANOVA ($p < 0.001$, $R=0.557$). Each treatment group represents 5 individual mosquito
888 midguts. For more information see also Supplementary Fig. 3.

889

890 **Fig. 4. Glyphosate Inhibits in vitro Melanin Production.** (A) An overall schematic of the

891 Mason-Raper pathway of melanization mediated by tyrosinase and auto-oxidation. (B)

892 Glyphosate inhibits formation of dopaquinone produced by tyrosinase-mediated and
893 spontaneous oxidation of L-DOPA. Dopaquinone is indicated by the absorbance of an MBTH-
894 Dopaquinone adduct pigment at 505 nm. Absorption levels are shown relative to the no
895 glyphosate control with background (MBTH mixture) subtracted after 1 h at 30°C **(C)** Glyphosate
896 decreases the rate of dopachrome formation and inhibits dopachrome production from
897 tyrosinase oxidation of L-DOPA. Rate of dopachrome formation is the reaction V_{max} at 490 nm
898 relative to the V_{max} without glyphosate. Dopachrome production is shown as the absorbance at
899 490 nm relative to the control after 30 min of reaction. **(D)** Melanin production is inhibited by
900 glyphosate with tyrosinase and auto-oxidation of L-DOPA. Melanin levels are measured as the
901 absorbance at 490 nm after 5 d of reaction. Inset shows a representative image of the data in
902 **(D)** showing melanization inhibition with increasing glyphosate concentration. Values are
903 depicted relative to the no glyphosate control. Error bars represent \pm SD. Each experiment was
904 performed at least three independent replicates.

905

906 **Fig. 5. Phosphate-Containing Compounds Inhibited Melanization Similarly to Glyphosate.**

907 Glyphosate, *o*-phosphoserine (PS), phosphonoacetic acid (PAA), pyrophosphate (pyro), and
908 phosphoric acid (PA) inhibit dopaquinone formation **(A)**, rate of dopachrome formation **(B)** and
909 dopachrome levels **(C)**, and melanin formation **(D)**, whereas their respective non-phosphate
910 analogs, glycine (gly), serine (ser), and acetic acid (AA) do not inhibit any step of melanization
911 **(A-D)**. **(E)** Auto-oxidation of L-DOPA is inhibited by glyphosate, PS, PAA, Pyro, and PA in a
912 similar manner. The compounds tested **(F)** were diluted in 300 mM stock solution and titrated to
913 pH between 5 and 6. Absorption and rates are shown relative to the internal no drug control.
914 Grayscale bars represent mean absorbance at 490 nm relative to no compound control. The
915 darker colors correspond to increased pigment formation. Inset shows a representative image of
916 the data in **(E)** showing the effects of the compounds on auto-oxidation. Error bars in **(A-C)**
917 represent \pm SD. Each experiment represents at least three independent replicates.

918

919 **Fig. 6. Glyphosate Does Not Directly Inhibit Tyrosinase Activity (A).** Tyrosinase activity is
920 not irreversibly inhibited and glyphosate-treated enzyme has normal activity when glyphosate is
921 dialyzed out of solution. **(B).** Glyphosate appears as a non-competitive inhibitor of tyrosinase in
922 Michaelis-Menten kinetics assays measuring the change in absorbance at 490 nm over 24 h
923 compared to the no tyrosinase background. **(C)** The rate of dopachrome formation with
924 glyphosate treatment is smaller than the slope of the control treatment across all concentrations
925 of tyrosinase. This reduced slope indicates reversible inhibition. The assay is performed under
926 constant L-DOPA and glyphosate concentrations. Shaded areas represent the 95% CI of the
927 linear regression **(D)** Adding Cu^{+2} to L-DOPA-tyrosinase reactions with glyphosate does not
928 rescue melanin inhibition compared to the glyphosate-free control. (See also Supplementary Fig.
929 5) Grayscale bars represent mean absorbance at 490 nm relative to no glyphosate and no
930 copper control. The darker colors correspond to increased pigment formation. Error bars in **(A-**
931 **C)** represent \pm SD. Each experiment represents at least three independent replicates.

932

933 **Fig. 7. Glyphosate Affects the Oxidative Properties of Melanogenesis. (A)** None of the
934 melanin inhibitors exhibit radical quenching properties in an ABTS assay aside from glyphosate,
935 which shows weak antioxidant properties after several hours in the ABTS solution. Absorbance at
936 734 nm is an indicator of how much ABTS remains in radical form (not quenched). **(B-C)** Citric acid
937 (CA), a non-radical quenching antioxidant (antioxidant synergist) exhibits similar melanin inhibition
938 as glyphosate and phosphoric acid, another known antioxidant synergist. Grayscale bars in **(C)**
939 represent absorbance at 490 nm relative to no compound control, with the darker colors
940 correspond to increased pigment formation. **(D)** Glyphosate, phosphoserine, phosphoric acid, and
941 citric acid show synergy with the antioxidant L-DOPA. The addition of these compounds to L-DOPA
942 enhances its radical quenching abilities by approximately 50%. Black dotted line represents the
943 normalized ABTS absorbance treated with water. The other compounds tested here alone do not

944 show much deviation from this line. The blue dotted line indicates the ABTS solution treated with L-
945 DOPA alone. ABTS treated with L-DOPA and synergetic compounds together are below this line. **(E)**
946 Average cyclic voltammogram showing the changes in oxidation and reduction of L-DOPA and
947 dopaquinone when exposed to 16 mM glyphosate but not water. Numbers correspond to shifted
948 peaks or peaks with less current compared to the water control. Peak 1 corresponds to L-DOPA
949 oxidation **(F)**; Peak 2 likely corresponds to dopaquinone reduction **(G)**. glyphosate shifts Peak 1 and
950 2 toward a decreased redox potential and diminishes the current of Peak 1 and 2 in a dose-
951 dependent manner **(H)** - notably decreasing Peak 2 current intensity to the point of non-existence
952 **(I)**. Each experiment represents at least three independent replicates. Error bars in **(A-B, D)**
953 represent \pm SD. See also Supplementary Fig. 6 and 8 .

954

955 **Supplementary Fig. 1. *G. mellonella* Supplemental Data. (A)** Broad-spectrum protease
956 inhibitor (cOmplete, Roche) was added to *G. mellonella* hemolymph to prevent the activation of
957 new phenoloxidase, and to control for any impact that glyphosate may have on phenoloxidase
958 activation cascade, cell viability, and gene expression. The general trend remains the same that
959 glyphosate inhibits phenoloxidase activity with and without protease inhibitor, albeit lower with
960 protease inhibitor due to the lower concentration of activated enzyme. **(B)** Phenoloxidase
961 activity was assessed using exogenous L-DOPA for one batch of *G. mellonella*, during these
962 experiments, the lower concentration of glyphosate resulted in increased phenoloxidase activity
963 as compared to the control. This suggests that there may be some cellular regulation of
964 phenoloxidase induced by glyphosate. It is possible that the doses of glyphosate tested elicit
965 some cellular response that increases phenoloxidase expression, secretion, and/or activation as
966 a feedback/hormesis-like response to the reduced melanin production. These data represent
967 three independent replicates, but this pattern of enzymatic activity as a function of glyphosate
968 concentration was not seen in subsequent batches of larvae. **(C)** Hemocyte viability was not
969 dramatically affected by concentrations of glyphosate ranging from 100 μ M to 10 mM, indicating

970 that our data are likely not artifacts of cytotoxic concentrations of glyphosate. Error bars in **(A-C)**
971 represent \pm SD. **(D)** AMPA, a major metabolite of glyphosate, inhibits tyrosinase-mediated
972 melanization similar to glyphosate. Grayscale bars represent mean absorbance at 490 nm
973 relative to no compound control. The darker colors correspond to increased pigment formation.
974 **(E)** Larvae treated with glyphosate and subsequently infected with *lac1* Δ mutant *C. neoformans*
975 strain showed a similar pattern of increased susceptibility as the wild type H99, although the
976 differences in susceptibility with the *lac1* Δ infected larvae are not statistically significant. Each
977 experiment represents at least three independent replicates. The PBS mock infection condition
978 represents survival of 95 animals, over the span of four biological replicates, and six total
979 technical replicates. The *lac1* Δ mutant infection represents survival of 75 animals over the span
980 of four biological replicates. The PBS mock infection data is the same as the data in Fig. 5b, as
981 all the infections were done concurrently under the same conditions. **(F)** Single injection of 10 μ l
982 of 1mM glyphosate does not affect the pupation of *G. mellonella* at 30°C and room temperature
983 (RT). Data from 30°C represents 25-35 animals for each group over two biological replicates,
984 and data from RT represents 45 animals from each group over three biological replicates.
985 Statistical analysis performed using Log-rank Mantel-Cox tests. **(G-I)** The three individual
986 replicates from **Fig. 1D** showing the size of the dark melanized particles within nodules are
987 significantly smaller in the glyphosate-treated infected groups compared to the PBS-treated
988 infected groups, with **(G)** and **(H)** showing that there were more melanized spots in the PBS-
989 treated infected group compared to the glyphosate-treated. All statistical analyses performed
990 using GraphPad Prism version 8.4.3 for Mac OS, GraphPad Software, San Diego California
991 USA, www.graphpad.com.

992

993 **Supplementary Fig. 2 Low efficiency *Plasmodium falciparum* infection of *A. gambiae* and**
994 **effects on mosquito cuticle (A).** Oocyst count per midgut for mosquitoes treated with or
995 without glyphosate and infected with high-passage *Plasmodium falciparum* gametocyte culture,

996 resulting in a low efficiency infection. Data represents one biological replicate. Dotted black line
997 indicates $y=0$. Black lines for each condition indicate median oocyst count per midgut. We have
998 chosen not to include the data from this replicate in the data shown in Fig. 6, because the
999 results from this one-off replicate appear due to poorly infectious parasite culture. Additionally, it
1000 is difficult to make comparisons using the low infection burden of the control group with a with
1001 the treatment groups, as well other replicates with higher oocyst burdens. **(B)** Infection
1002 prevalence (percent midguts with at least one oocyst) from the experiment described in **(A)**.
1003 Fisher's Exact test performed for each condition individually compared to control and corrected
1004 for multiple comparisons using the Bonferroni method. **(C)** 5 days of 1 mM glyphosate treatment
1005 in adult female mosquitoes does not influence the abdomen's cuticular darkness as measured
1006 by mean gray value with 0 being pure black and 255 being pure white. Data representative of 2
1007 biological replicates with 88 mosquitoes measured per condition. **(D)** Wing length, as a proxy for
1008 body mass and size, is not affected by 5 days of glyphosate treatment. Data representative of a
1009 single biological replicates with 32-36 mosquitoes measured per condition. Line and error bar
1010 represent mean \pm SD in **(C-D)**. Unpaired t-test performed to determine statistical significance in
1011 **(C-D)**. All statistical analyses performed using GraphPad Prism version 8.4.3 for Mac OS,
1012 GraphPad Software, San Diego California USA, www.graphpad.com.

1013

1014 **Supplementary Fig. 3. *Glyphosate affects the *A. gambiae* microbiota in a dose-***

1015 ***independent manner*** **(A)** At the class level, glyphosate leads to an enrichment of
1016 Alphaproteobacteria and a depletion in Gammaproteobacteria. Tables showing the relative
1017 abundance of bacterial classes **(B)** and individual bacterial genera **(C)** following glyphosate
1018 treatment. **(D)** Alpha diversity does not follow a distinctive pattern with increasing glyphosate
1019 dose. **(E)** Glyphosate-treated and control-treated microbiota cluster separately in ordination
1020 space, but the clusters are not dose-dependent.

1021

1022 **Supplementary Fig 4. Reaction of glyphosate with L-DOPA.** Representative ^1H NMR spectra
1023 of 60 mM glyphosate solution in D_2O (**Green**), 20 mM L-DOPA solution in D_2O (**Red**), and 20
1024 mM L-DOPA mixed with 60 mM glyphosate in D_2O (**Blue**). There appears to be no shift in ^1H
1025 peaks and no appearance of new peaks, which is indicative of no reaction occurring between
1026 the compounds. Data representative of three independent replicates

1027
1028 **Supplementary Fig. 5. Glyphosate appears to “buffer” copper concentration in solution.**
1029 High doses (2-16 mM) of glyphosate prevent the enzymatic activity enhancing effects of lower
1030 copper concentration (6.25-25 μM), but high doses of glyphosate also prevent the enzyme
1031 inhibitory effects of high copper concentration (100-400 μM). Error bars represent $\pm\text{SD}$. Data
1032 represents at least three independent replicates.

1033
1034 **Supplementary Fig. 6. Antioxidant Properties of glyphosate. (A)** Change in absorbance of
1035 ABTS solution at 734 nm over time for 33.33 mM glyphosate relative to the no glyphosate
1036 control. This indicates glyphosate quenches free radicals over an extended period of time. **(B)**
1037 Calculated antioxidant radical scavenging synergy between compounds tested and L-DOPA.
1038 Values represent the mean of at least three independent replicates. Error bars represent $\pm\text{SD}$.

1039
1040 **Supplementary Fig. 7. Glyphosate inhibits melanin production independent of L-DOPA**
1041 **concentration. (A)** Inhibitory concentrations of glyphosate are not affected by L-DOPA
1042 concentration. This indicates that glyphosate is not reacting proportionately with L-DOPA as
1043 measured by absorbance at 490 nm after 5 d of reaction, relative to the no glyphosate control
1044 and with background absorbance subtracted. **(B)** The IC_{50} of glyphosate remains constant at
1045 approximately 1 mM relative inhibition of melanin production appears dependent on glyphosate
1046 concentration alone, and not on L-DOPA to glyphosate ratio. Error bars represent $\pm\text{SD}$. Each
1047 experiment represents at least three independent replicates. Grayscale bars represent mean

1048 absorbance at 490 nm relative to no compound control. The darker colors correspond to
1049 increased pigment formation. Red line represents the approximate IC₅₀. Crossed out boxes
1050 represent values with no data.

1051

1052 **Supplementary Fig. 8. Cyclic Voltammetry Supplemental Data. (A)** Peak 1 was validated as
1053 the oxidation of L-DOPA, and Peak 2 was validated as the reduction peak of dopaquinone by
1054 correlating increased peak intensity with increasing concentration of L-DOPA under the same
1055 potentiostat parameters. **(B)** Glycine (16 mM) – a non-phosphate analog of glyphosate, a non-
1056 inhibitor of melanization, and a non-antioxidant - does not alter the oxidation potential of L-
1057 DOPA. Conversely, Citric Acid (16 mM) – a known synergistic antioxidant and inhibitor of
1058 melanization – does alter the oxidation potential of L-DOPA in similar ways as glyphosate. Each
1059 experiment represents at least three independent replicates, with three cycles per replicate. The
1060 tracings represent the mean value of the three replicates over the course of three cycles.

1061

1062 **Supplementary Fig. 9. Experimental Methods Diagram for Insect Experiments. (A).** During *G.*
1063 *mellonella* infection with *C. neoformans*, larvae were injected with 10 µl of 1 mM glyphosate, left to
1064 recover for 5 h, and were subsequently infected with 10⁴ cells/larvae of *C. neoformans* H99 strain.
1065 Survival was monitored for 14 days. **(B)** During *A. gambiae* infection with *P. falciparum*, mosquitoes
1066 were drugged with glyphosate-laced 10% sucrose solution for 5 days, then fed with a *P. falciparum*-
1067 infected blood meal, and fed 10% sucrose for 8 d. On Day 8, mosquitoes were dissected, and the
1068 midguts were stained with mercurochrome to facilitate oocyst enumeration. **(C)** glyphosate-drugged
1069 mosquitoes were dissected under sterile conditions, and five midguts were collected individually per
1070 condition. DNA was extracted from samples and bacterial 16S rRNA genes were amplified by PCR
1071 and sample-specific Illumina adapters were ligated to products. PCR products were pooled and
1072 sequenced on the Illumina MiSeq platform. Data were then analyzed using mothur to construct
1073 contigs, align reads, remove ambiguous bases and chimeric regions, align sequences to the Silva

1074 16S V4 reference database, and cluster reads into 3% operational taxonomic units (OTUs).
1075 Sequences from known contaminants were removed. Alpha and beta diversity measurements were
1076 performed using the Shannon diversity index and Bray-Curtis dissimilarity distance respectively and
1077 plotted using MicrobiomeAnalyst. Figures made with BioRender.

1078

1079 **REFERENCES:**

- 1080 1. Whitten MMA, Coates CJ. Re-evaluation of insect melanogenesis research: Views from
1081 the dark side. *Pigment Cell & Melanoma Research*. 2017;30(4):386–401.
- 1082 2. Prota G. Recent Advances in the Chemistry of Melanogenesis in Mammals. *Journal of*
1083 *Investigative Dermatology*. 1980 Jul 1;75(1):122–7.
- 1084 3. Nappi AJ, Christensen BM. Melanogenesis and associated cytotoxic reactions:
1085 Applications to insect innate immunity. *Insect Biochemistry and Molecular Biology*.
1086 2005 May 1;35(5):443–59.
- 1087 4. Fujieda N, Murata M, Yabuta S, Ikeda T, Shimokawa C, Nakamura Y, et al. Multifunctions
1088 of MelB, a Fungal Tyrosinase from *Aspergillus oryzae*. *ChemBioChem*.
1089 2012;13(2):193–201.
- 1090 5. Lerch K. Tyrosinase: Molecular and Active-Site Structure. In: *Enzymatic Browning and*
1091 *Its Prevention* [Internet]. American Chemical Society; 1995 [cited 2020 Oct 21]. p.
1092 64–80. (ACS Symposium Series; vol. 600). Available from:
1093 <https://doi.org/10.1021/bk-1995-0600.ch005>
- 1094 6. Galván I, Solano F. Bird Integumentary Melanins: Biosynthesis, Forms, Function and
1095 Evolution. *International Journal of Molecular Sciences*. 2016 Apr;17(4):520.
- 1096 7. Martín-Durán JM, de Mendoza A, Sebé-Pedrós A, Ruiz-Trillo I, Hejnol A. A Broad
1097 Genomic Survey Reveals Multiple Origins and Frequent Losses in the Evolution of
1098 Respiratory Hemerythrins and Hemocyanins. *Genome Biol Evol*. 2013 Jul
1099 1;5(7):1435–42.
- 1100 8. Ramsden CA, Riley PA. Tyrosinase: The four oxidation states of the active site and their
1101 relevance to enzymatic activation, oxidation and inactivation. *Bioorganic & Medicinal*
1102 *Chemistry*. 2014 Apr 15;22(8):2388–95.
- 1103 9. Christensen BM, Li J, Chen C-C, Nappi AJ. Melanization immune responses in mosquito
1104 vectors. *Trends in Parasitology*. 2005 Apr 1;21(4):192–9.
- 1105 10. González-Santoyo I, Córdoba-Aguilar A. Phenoloxidase: a key component of the insect
1106 immune system. *Entomologia Experimentalis et Applicata*. 2012;142(1):1–16.

- 1107 11. Marmaras VJ, Charalambidis ND, Zervas CG. Immune response in insects: the role of
1108 phenoloxidase in defense reactions in relation to melanization and sclerotization.
1109 Arch Insect Biochem Physiol. 1996;31(2):119–33.
- 1110 12. Chen CC, Chen CS. *Brugia bahangi*: Effects of Melanization on the Uptake of Nutrients by
1111 Microfilariae in Vitro. Experimental Parasitology. 1995 Aug 1;81(1):72–8.
- 1112 13. Zhao P, Lu Z, Strand MR, Jiang H. Antiviral, anti-parasitic, and cytotoxic effects of 5,6-
1113 dihydroxyindole (DHI), a reactive compound generated by phenoloxidase during
1114 insect immune response. Insect Biochem Mol Biol. 2011 Sep;41(9):645–52.
- 1115 14. Ezzati-Tabizi R, Talaei-Hassanloui R, Farrokhi N, Hossininaveh V, Alavi M. Haemolymph
1116 phenoloxidase activity of larval *Plodia interpunctella* and *Galleria mellonella* in
1117 response to *Beauveria bassiana* and *Pseudomonas fluorescens*. International Journal
1118 of Agriculture Innovations and Research. 2013;2(2):217–20.
- 1119 15. Vertyporokh L, Hulaś-Stasiak M, Wojda I. Host–pathogen interaction after infection of
1120 *Galleria mellonella* with the filamentous fungus *Beauveria bassiana*. Insect Science.
1121 2020;27(5):1079–89.
- 1122 16. Nayar JK (University of F, Knight JW. Wounding increases intracellular encapsulation
1123 (melanization) of developing *Brugia malayi* (Nematoda: Filarioidea) larvae in
1124 thoracic muscles of *Anopheles quadrimaculatus*. Comparative biochemistry and
1125 physiology Part A, Physiology (USA) [Internet]. 1995 [cited 2020 Oct 21]; Available
1126 from: <https://agris.fao.org/agris-search/search.do?recordID=US9619494>
- 1127 17. Nayar JK, Knight JW, Vickery AC. Intracellular Melanization in the Mosquito *Anopheles*
1128 *quadrimaculatus* (Diptera: Culicidae) Against the Filarial Nematodes, *Brugia* spp.
1129 (Nematoda: Filarioidea). J Med Entomol. 1989 May 1;26(3):159–66.
- 1130 18. Yassine H, Kamareddine L, Osta MA. The Mosquito Melanization Response Is Implicated
1131 in Defense against the Entomopathogenic Fungus *Beauveria bassiana*. PLOS
1132 Pathogens. 2012 Nov 15;8(11):e1003029.
- 1133 19. Zdybicka-Barabas A, Cytryńska M. Phenoloxidase activity in hemolymph of *Galleria*
1134 *mellonella* larvae challenged with *Aspergillus oryzae*. 2011 [cited 2020 Oct 21];
1135 Available from: <https://pubag.nal.usda.gov/catalog/5208902>
- 1136 20. Dimopoulos G, Müller H-M, Levashina EA, Kafatos FC. Innate immune defense against
1137 malaria infection in the mosquito. Current Opinion in Immunology. 2001 Feb
1138 1;13(1):79–88.
- 1139 21. Schnitger AKD, Kafatos FC, Osta MA. The Melanization Reaction Is Not Required for
1140 Survival of *Anopheles gambiae* Mosquitoes after Bacterial Infections. J Biol Chem.
1141 2007 Jul 27;282(30):21884–8.

- 1142 22. Dubovskiy IM, Kryukova NA, Glupov VV, Ratcliffe NA. Encapsulation and nodulation in
1143 insects. *Invertebrate Survival Journal*. 2016 Jul 7;13(1):229–46.
- 1144 23. Du M-H, Yan Z-W, Hao Y-J, Yan Z-T, Si F-L, Chen B, et al. Suppression of Laccase 2
1145 severely impairs cuticle tanning and pathogen resistance during the pupal
1146 metamorphosis of *Anopheles sinensis* (Diptera: Culicidae). *Parasites Vectors*. 2017
1147 Apr 4;10(1):171.
- 1148 24. Qiao L, Du M, Liang X, Hao Y, He X, Si F, et al. Tyrosine Hydroxylase is crucial for
1149 maintaining pupal tanning and immunity in *Anopheles sinensis*. *Scientific Reports*.
1150 2016 Jul 15;6(1):29835.
- 1151 25. Goulson D. The insect apocalypse, and why it matters. *Current Biology*. 2019 Oct
1152 7;29(19):R967–71.
- 1153 26. Nosanchuk JD, Ovalle R, Casadevall A. Glyphosate Inhibits Melanization of *Cryptococcus*
1154 *neoformans* and Prolongs Survival of Mice after Systemic Infection. *J Infect Dis*. 2001
1155 Apr 1;183(7):1093–9.
- 1156 27. Samsel A, Seneff S. Glyphosate pathways to modern diseases V: Amino acid analogue of
1157 glycine in diverse proteins. *Journal of Biological Physics and Chemistry*. 2016 Mar
1158 30;16(1):9–46.
- 1159 28. Duke SO, Powles SB. Glyphosate: a once-in-a-century herbicide. *Pest Management*
1160 *Science*. 2008;64(4):319–25.
- 1161 29. Dill GM. Glyphosate-resistant crops: history, status and future. *Pest Management*
1162 *Science*. 2008;61(3):219–24.
- 1163 30. Gianessi JC & L. Herbicide Tolerant Soybeans: Why Growers Are Adopting Roundup
1164 Ready Varieties [Internet]. 1999 [cited 2018 Jun 20]. Available from:
1165 <http://agbioforum.org/v2n2/v2n2a02-carpenter.htm>
- 1166 31. Benbrook CM. Impacts of genetically engineered crops on pesticide use in the U.S. -- the
1167 first sixteen years. *Environ Sci Eur*. 2012 Dec 1;24(1):24.
- 1168 32. Benbrook CM. Trends in glyphosate herbicide use in the United States and globally.
1169 *Environ Sci Eur* [Internet]. 2016 [cited 2018 Jun 20];28(1). Available from:
1170 <https://www.ncbi.nlm.nih.gov/pmc/articles/PMC5044953/>
- 1171 33. Bott S, Tesfamariam T, Candan H, Cakmak I, Römheld V, Neumann G. Glyphosate-
1172 induced impairment of plant growth and micronutrient status in glyphosate-resistant
1173 soybean (*Glycine max* L.). *Plant Soil*. 2008 Sep 11;312(1):185.
- 1174 34. Laitinen P, Rämö S, Siimes K. Glyphosate translocation from plants to soil – does this
1175 constitute a significant proportion of residues in soil? *Plant Soil*. 2007 Nov
1176 1;300(1):51–60.

- 1177 35. Singh S, Kumar V, Datta S, Wani AB, Dhanjal DS, Romero R, et al. Glyphosate uptake,
1178 translocation, resistance emergence in crops, analytical monitoring, toxicity and
1179 degradation: a review. *Environ Chem Lett*. 2020 May 1;18(3):663–702.
- 1180 36. Laitinen P, Siimes K, Rämö S, Jauhiainen L, Eronen L, Oinonen S, et al. Effects of Soil
1181 Phosphorus Status on Environmental Risk Assessment of Glyphosate and
1182 Glufosinate-Ammonium. *Journal of Environmental Quality*. 2008;37(3):830–8.
- 1183 37. Laitinen P, Rämö S, Nikunen U, Jauhiainen L, Siimes K, Turtola E. Glyphosate and
1184 phosphorus leaching and residues in boreal sandy soil. *Plant Soil*. 2009 Oct
1185 1;323(1):267–83.
- 1186 38. Lupi L, Bedmar F, Puricelli M, Marino D, Aparicio VC, Wunderlin D, et al. Glyphosate
1187 runoff and its occurrence in rainwater and subsurface soil in the nearby area of
1188 agricultural fields in Argentina. *Chemosphere*. 2019 Jun 1;225:906–14.
- 1189 39. Edwards WM, Triplett GB, Kramer RM. A Watershed Study of Glyphosate Transport in
1190 Runoff 1. *Journal of Environmental Quality*. 1980 12/01;9(4):661–5.
- 1191 40. Silva V, Montanarella L, Jones A, Fernández-Ugalde O, Mol HGJ, Ritsema CJ, et al.
1192 Distribution of glyphosate and aminomethylphosphonic acid (AMPA) in agricultural
1193 topsoils of the European Union. *Science of The Total Environment*. 2018 Apr
1194 15;621:1352–9.
- 1195 41. Battaglin WA, Meyer MT, Kuivila KM, Dietze JE. Glyphosate and Its Degradation Product
1196 AMPA Occur Frequently and Widely in U.S. Soils, Surface Water, Groundwater, and
1197 Precipitation. *JAWRA Journal of the American Water Resources Association*.
1198 2014;50(2):275–90.
- 1199 42. Bento CPM, Yang X, Gort G, Xue S, van Dam R, Zomer P, et al. Persistence of glyphosate
1200 and aminomethylphosphonic acid in loess soil under different combinations of
1201 temperature, soil moisture and light/darkness. *Science of The Total Environment*.
1202 2016 Dec 1;572:301–11.
- 1203 43. Yang X, Wang F, Bento CPM, Meng L, van Dam R, Mol H, et al. Decay characteristics and
1204 erosion-related transport of glyphosate in Chinese loess soil under field conditions.
1205 *Science of The Total Environment*. 2015 Oct 15;530–531:87–95.
- 1206 44. Laitinen P, Siimes K, Eronen L, Rämö S, Welling L, Oinonen S, et al. Fate of the herbicides
1207 glyphosate, glufosinate-ammonium, phenmedipham, ethofumesate and metamitron
1208 in two Finnish arable soils. *Pest Management Science*. 2006;62(6):473–91.
- 1209 45. Sviridov AV. Microbial degradation of glyphosate herbicides (Review). *Applied
1210 biochemistry and microbiology*. 2015 Mar;v. 51(2):188–95.
- 1211 46. Gill JPK, Sethi N, Mohan A, Datta S, Girdhar M. Glyphosate toxicity for animals. *Environ
1212 Chem Lett*. 2018 Jun 1;16(2):401–26.

- 1213 47. Druille M, Cabello MN, Omacini M, Golluscio RA. Glyphosate reduces spore viability and
1214 root colonization of arbuscular mycorrhizal fungi. *Applied Soil Ecology*. 2013 Feb
1215 1;64:99–103.
- 1216 48. Schafer JR, Hallett SG, Johnson WG. Rhizosphere Microbial Community Dynamics in
1217 Glyphosate-Treated Susceptible and Resistant Biotypes of Giant Ragweed (*Ambrosia*
1218 *trifida*). *wees*. 2014 Apr;62(2):370–81.
- 1219 49. Zobiolo LHS, Kremer RJ, Oliveira RS, Constantin J. Glyphosate affects micro-organisms
1220 in rhizospheres of glyphosate-resistant soybeans. *Journal of Applied Microbiology*.
1221 2011;110(1):118–27.
- 1222 50. Van Bruggen AHC, He MM, Shin K, Mai V, Jeong KC, Finckh MR, et al. Environmental and
1223 health effects of the herbicide glyphosate. *Science of The Total Environment*. 2018
1224 Mar 1;616–617:255–68.
- 1225 51. Ratcliff AW, Busse MD, Shestak CJ. Changes in microbial community structure following
1226 herbicide (glyphosate) additions to forest soils. *Applied Soil Ecology*. 2006 Dec
1227 1;34(2):114–24.
- 1228 52. Busse MD, Ratcliff AW, Shestak CJ, Powers RF. Glyphosate toxicity and the effects of
1229 long-term vegetation control on soil microbial communities. *Soil Biology and*
1230 *Biochemistry*. 2001 Oct 1;33(12):1777–89.
- 1231 53. Weaver MA, Krutz LJ, Zablutowicz RM, Reddy KN. Effects of glyphosate on soil microbial
1232 communities and its mineralization in a Mississippi soil. *Pest Management Science*.
1233 2007;63(4):388–93.
- 1234 54. Pochron S, Simon L, Mirza A, Littleton A, Sahebzada F, Yudell M. Glyphosate but not
1235 Roundup harms earthworms (*Eisenia fetida*). *Chemosphere*. 2020 Feb 1;241:125017.
- 1236 55. Krams IA, Kecko S, Jõers P, Trakimas G, Elferts D, Krams R, et al. Microbiome symbionts
1237 and diet diversity incur costs on the immune system of insect larvae. *Journal of*
1238 *Experimental Biology*. 2017 Nov 15;220(22):4204–12.
- 1239 56. Lewis Z, Lizé A. Insect behaviour and the microbiome. *Current Opinion in Insect*
1240 *Science*. 2015 Jun 1;9:86–90.
- 1241 57. Weiss B, Aksoy S. Microbiome influences on insect host vector competence. *Trends in*
1242 *Parasitology*. 2011 Nov 1;27(11):514–22.
- 1243 58. Lesperance DN, Broderick NA. Microbiomes as modulators of *Drosophila melanogaster*
1244 homeostasis and disease. *Current Opinion in Insect Science*. 2020 Jun 1;39:84–90.
- 1245 59. Motta EVS, Raymann K, Moran NA. Glyphosate perturbs the gut microbiota of honey
1246 bees. *Proc Natl Acad Sci USA*. 2018 09;115(41):10305–10.

- 1247 60. Blot N, Veillat L, Rouzé R, Delatte H. Glyphosate, but not its metabolite AMPA, alters the
1248 honeybee gut microbiota. *PLOS ONE*. 2019 Apr 16;14(4):e0215466.
- 1249 61. Rio RVM, Jozwick AKS, Savage AF, Sabet A, Vigneron A, Wu Y, et al. Mutualist-
1250 Provisioned Resources Impact Vector Competency. *mBio*. 2019 Jun 25;10(3):e00018-
1251 19.
- 1252 62. Houghton AJ, Bell JR, Wilcox A, Boatman ND. The effect of the herbicide glyphosate on
1253 non-target spiders: Part I. Direct effects on *Lepthyphantes tenuis* under laboratory
1254 conditions. *Pest Management Science*. 2001;57(11):1033–6.
- 1255 63. Evans SC, Shaw EM, Rypstra AL. Exposure to a glyphosate-based herbicide affects
1256 agrobiont predatory arthropod behaviour and long-term survival. *Ecotoxicology*.
1257 2010 Oct 1;19(7):1249–57.
- 1258 64. Tahir HM, Basheer T, Ali S, Yaqoob R, Naseem S, Khan SY. Effect of Pesticides on
1259 Biological Control Potential of *Neoscona theisi* (Araneae: Araneidae). *J Insect Sci*
1260 [Internet]. 2019 Mar 1 [cited 2020 Oct 18];19(2). Available from:
1261 <https://academic.oup.com/jinsectscience/article/19/2/17/5420491>
- 1262 65. Baglan H, Lazzari CR, Guerrieri FJ. Glyphosate impairs learning in *Aedes aegypti*
1263 mosquito larvae at field-realistic doses. *Journal of Experimental Biology* [Internet].
1264 2018 Oct 15 [cited 2020 Oct 14];221(20). Available from:
1265 <https://jeb.biologists.org/content/221/20/jeb187518>
- 1266 66. Farina WM, Balbuena MS, Herbert LT, Mengoni Goñalons C, Vázquez DE. Effects of the
1267 Herbicide Glyphosate on Honey Bee Sensory and Cognitive Abilities: Individual
1268 Impairments with Implications for the Hive. *Insects*. 2019 Oct;10(10):354.
- 1269 67. Tomé HVV, Schmehl DR, Wedde AE, Godoy RSM, Ravaiano SV, Guedes RNC, et al.
1270 Frequently encountered pesticides can cause multiple disorders in developing
1271 worker honey bees. *Environmental Pollution*. 2020 Jan 1;256:113420.
- 1272 68. Cuhra M, Traavik T, Dando M, Primicerio R, Holderbaum DF, Bøhn T. Glyphosate-
1273 Residues in Roundup-Ready Soybean Impair *Daphnia magna* Life-Cycle. *Journal of*
1274 *Agricultural Chemistry and Environment*. 2015 Jan 22;4(1):24–36.
- 1275 69. Güngördü A. Comparative toxicity of methidathion and glyphosate on early life stages of
1276 three amphibian species: *Pelophylax ridibundus*, *Pseudepidalea viridis*, and *Xenopus*
1277 *laevis*. *Aquatic Toxicology*. 2013 Sep 15;140–141:220–8.
- 1278 70. El-Shenawy NS. Oxidative stress responses of rats exposed to Roundup and its active
1279 ingredient glyphosate. *Environmental Toxicology and Pharmacology*. 2009 Nov
1280 1;28(3):379–85.

- 1281 71. Uren Webster TM, Santos EM. Global transcriptomic profiling demonstrates induction
1282 of oxidative stress and of compensatory cellular stress responses in brown trout
1283 exposed to glyphosate and Roundup. *BMC Genomics*. 2015 Jan 31;16(1):32.
- 1284 72. Nwani CD, Nagpure NS, Kumar R, Kushwaha B, Lakra WS. DNA damage and oxidative
1285 stress modulatory effects of glyphosate-based herbicide in freshwater fish, *Channa*
1286 *punctatus*. *Environmental Toxicology and Pharmacology*. 2013 Sep 1;36(2):539–47.
- 1287 73. de Aguiar LM, Figueira FH, Gottschalk MS, da Rosa CE. Glyphosate-based herbicide
1288 exposure causes antioxidant defence responses in the fruit fly *Drosophila*
1289 *melanogaster*. *Comparative Biochemistry and Physiology Part C: Toxicology &*
1290 *Pharmacology*. 2016 Jul 1;185–186:94–101.
- 1291 74. Puértolas L, Damásio J, Barata C, Soares AMVM, Prat N. Evaluation of side-effects of
1292 glyphosate mediated control of giant reed (*Arundo donax*) on the structure and
1293 function of a nearby Mediterranean river ecosystem. *Environmental Research*. 2010
1294 Aug 1;110(6):556–64.
- 1295 75. Kwiatkowska M, Nowacka-Krukowska H, Bukowska B. The effect of glyphosate, its
1296 metabolites and impurities on erythrocyte acetylcholinesterase activity.
1297 *Environmental Toxicology and Pharmacology*. 2014 May 1;37(3):1101–8.
- 1298 76. Kwiatkowska M, Huras B, Bukowska B. The effect of metabolites and impurities of
1299 glyphosate on human erythrocytes (in vitro). *Pesticide Biochemistry and Physiology*.
1300 2014 Feb 1;109:34–43.
- 1301 77. González-Santoyo I, Córdoba-Aguilar A. Phenoloxidase: a key component of the insect
1302 immune system. *Entomologia Experimentalis et Applicata*. 2012;142(1):1–16.
- 1303 78. Mylonakis E, Moreno R, Khoury JBE, Idnurm A, Heitman J, Calderwood SB, et al. *Galleria*
1304 *mellonella* as a Model System To Study *Cryptococcus neoformans* Pathogenesis.
1305 *Infection and Immunity*. 2005 Jul 1;73(7):3842–50.
- 1306 79. Smith RC, Vega-Rodríguez J, Jacobs-Lorena M, Smith RC, Vega-Rodríguez J, Jacobs-
1307 Lorena M. The Plasmodium bottleneck: malaria parasite losses in the mosquito
1308 vector. *Memórias do Instituto Oswaldo Cruz*. 2014 Aug;109(5):644–61.
- 1309 80. Sinden RE, Billingsley PF. Plasmodium invasion of mosquito cells: hawk or dove?
1310 *Trends Parasitol*. 2001 May;17(5):209–12.
- 1311 81. Whitten MMA, Shiao SH, Levashina EA. Mosquito midguts and malaria: cell biology,
1312 compartmentalization and immunology. *Parasite Immunology*. 2006;28(4):121–30.
- 1313 82. Gouagna LC, Gouagna LC, Mulder B, Mulder B, Noubissi E, Noubissi E, et al. The early
1314 sporogonic cycle of *Plasmodium falciparum* in laboratory-infected *Anopheles*
1315 *gambiae*: an estimation of parasite efficacy. *Tropical Medicine & International Health*.
1316 1998;3(1):21–8.

- 1317 83. Dong Y, Manfredini F, Dimopoulos G. Implication of the Mosquito Midgut Microbiota in
1318 the Defense against Malaria Parasites. *PLoS Pathog* [Internet]. 2009 May 8 [cited
1319 2020 Apr 4];5(5). Available from:
1320 <https://www.ncbi.nlm.nih.gov/pmc/articles/PMC2673032/>
- 1321 84. Bahia AC, Dong Y, Blumberg BJ, Mlambo G, Tripathi A, BenMarzouk-Hidalgo OJ, et al.
1322 Exploring Anopheles gut bacteria for Plasmodium blocking activity. *Environ*
1323 *Microbiol.* 2014 Sep;16(9):2980–94.
- 1324 85. Bai L, Wang L, Vega-Rodríguez J, Wang G, Wang S. A Gut Symbiotic Bacterium *Serratia*
1325 *marcescens* Renders Mosquito Resistance to Plasmodium Infection Through
1326 Activation of Mosquito Immune Responses. *Front Microbiol.* 2019;10:1580.
- 1327 86. Romoli O, Gendrin M. The tripartite interactions between the mosquito, its microbiota
1328 and Plasmodium. *Parasit Vectors.* 2018 20;11(1):200.
- 1329 87. Mason HS. The chemistry of melanin; mechanism of the oxidation of
1330 dihydroxyphenylalanine by tyrosinase. *J Biol Chem.* 1948 Jan;172(1):83–99.
- 1331 88. Raper HS. The Tyrosinase-tyrosine Reaction. *Biochem J.* 1927;21(1):89–96.
- 1332 89. García-Borrón JC, Sánchez MCO. Biosynthesis of Melanins. In: *Melanins and*
1333 *Melanosomes* [Internet]. John Wiley & Sons, Ltd; 2011 [cited 2019 Jun 8]. p. 87–116.
1334 Available from:
1335 <https://onlinelibrary.wiley.com/doi/abs/10.1002/9783527636150.ch4>
- 1336 90. Jara JR, Solano F, Lozano JA. Assays for Mammalian Tyrosinase: A Comparative Study.
1337 *Pigment Cell Research.* 1988;1(5):332–9.
- 1338 91. Chen Q-X, Song K-K, Wang Q, Huang H. Inhibitory Effects on Mushroom Tyrosinase by
1339 Some Alkylbenzaldehydes. *Journal of Enzyme Inhibition and Medicinal Chemistry.*
1340 2003 Dec 1;18(6):491–6.
- 1341 92. Liu H-J, Ji S, Fan Y-Q, Yan L, Yang J-M, Zhou H-M, et al. The Effect of D-(–)-arabinose on
1342 Tyrosinase: An Integrated Study Using Computational Simulation and Inhibition
1343 Kinetics [Internet]. Vol. 2012, *Enzyme Research.* Hindawi; 2012 [cited 2020 Oct 27].
1344 p. e731427. Available from: <https://www.hindawi.com/journals/er/2012/731427/>
- 1345 93. Glass RL. Metal complex formation by glyphosate. *J Agric Food Chem.* 1984 Nov
1346 1;32(6):1249–53.
- 1347 94. Madsen HEL, Christensen HH, Gottlieb-Petersen C, Andresen AF, Smidsrød O, Pontchour
1348 C-O, et al. Stability Constants of Copper(II), Zinc, Manganese(II), Calcium, and
1349 Magnesium Complexes of N-(Phosphonomethyl)glycine (Glyphosate). *Acta Chem*
1350 *Scand.* 1978;32a:79–83.

- 1351 95. Zhou C-F, Wang Y-J, Li C-C, Sun R-J, Yu Y-C, Zhou D-M. Subacute toxicity of copper and
1352 glyphosate and their interaction to earthworm (*Eisenia fetida*). *Environmental*
1353 *Pollution*. 2013 Sep 1;180:71–7.
- 1354 96. Riley PA. Radicals in Melanin Biochemistry a. *Annals of the New York Academy of*
1355 *Sciences*. 1988;551(1):111–9.
- 1356 97. Gordon MH. The Mechanism of Antioxidant Action in Vitro. In: Hudson BJF, editor. *Food*
1357 *Antioxidants* [Internet]. Dordrecht: Springer Netherlands; 1990 [cited 2019 Jun 8]. p.
1358 1–18. (Elsevier Applied Food Science Series). Available from:
1359 https://doi.org/10.1007/978-94-009-0753-9_1
- 1360 98. Choe E, Min DB. Mechanisms of Antioxidants in the Oxidation of Foods. *Comprehensive*
1361 *Reviews in Food Science and Food Safety*. 2009;8(4):345–58.
- 1362 99. Jodko-Piórecka K, Litwinienko G. Antioxidant activity of dopamine and L-DOPA in lipid
1363 micelles and their cooperation with an analogue of α -tocopherol. *Free Radical*
1364 *Biology and Medicine*. 2015 Jun 1;83:1–11.
- 1365 100. Bailey SI, Ritchie IM. A cyclic voltammetric study of the aqueous electrochemistry of
1366 some quinones. *Electrochimica Acta*. 1985 Jan 1;30(1):3–12.
- 1367 101. Kissinger PT, Heineman WR. Cyclic voltammetry. *J Chem Educ*. 1983 Sep 1;60(9):702.
- 1368 102. Liu X, Zhang Z, Cheng G, Dong S. Spectroelectrochemical and Voltammetric Studies of
1369 L-DOPA. *Electroanalysis*. 2003;15(2):103–7.
- 1370 103. Fotouhi L, Tammari E, Asadi S, Heravi MM, Nematollahi D. Estimation of
1371 heterogeneous rate constants of reaction of electrochemically generated o-
1372 benzoquinones with various nucleophiles containing thiol group. *International*
1373 *Journal of Chemical Kinetics*. 2009 Jun 1;41(6):426–31.
- 1374 104. Boyle JH, Dagleish HJ, Puzey JR. Monarch butterfly and milkweed declines
1375 substantially predate the use of genetically modified crops. *Proc Natl Acad Sci U S A*.
1376 2019 Feb 19;116(8):3006–11.
- 1377 105. Wepprich T, Adrion JR, Ries L, Wiedmann J, Haddad NM. Butterfly abundance
1378 declines over 20 years of systematic monitoring in Ohio, USA. *PLOS ONE*. 2019 Jul
1379 9;14(7):e0216270.
- 1380 106. Wepprich T. Monarch butterfly trends are sensitive to unexamined changes in
1381 museum collections over time. *PNAS*. 2019 Jul 9;116(28):13742–4.
- 1382 107. Thogmartin WE, Wiederholt R, Oberhauser K, Drum RG, Diffendorfer JE, Altizer S, et
1383 al. Monarch butterfly population decline in North America: identifying the
1384 threatening processes. *Royal Society Open Science*. 4(9):170760.

- 1385 108. Molina-Cruz A, DeJong RJ, Ortega C, Haile A, Abban E, Rodrigues J, et al. Some strains
1386 of *Plasmodium falciparum*, a human malaria parasite, evade the complement-like
1387 system of *Anopheles gambiae* mosquitoes. *PNAS*. 2012 Jul 10;109(28):E1957–62.
- 1388 109. Urabe K, Aroca P, Tsukamoto K, Mascagna D, Palumbo A, Prota G, et al. The inherent
1389 cytotoxicity of melanin precursors: A revision. *Biochimica et Biophysica Acta (BBA) -*
1390 *Molecular Cell Research*. 1994 Apr 28;1221(3):272–8.
- 1391 110. Smith RC, Barillas-Mury C. *Plasmodium* Oocysts: Overlooked Targets of Mosquito
1392 Immunity. *Trends Parasitol*. 2016;32(12):979–90.
- 1393 111. Hogg JC, Hurd H. The effects of natural *Plasmodium falciparum* infection on the
1394 fecundity and mortality of *Anopheles gambiae* s. l. in north east Tanzania.
1395 *Parasitology*. 1997 Apr;114 (Pt 4):325–31.
- 1396 112. Okech BA, Gouagna LC, Kabiru EW, Beier JC, Yan G, Githure JI. Influence of age and
1397 previous diet of *Anopheles gambiae* on the infectivity of natural *Plasmodium*
1398 *falciparum* gametocytes from human volunteers. *J Insect Sci* [Internet]. 2004 Oct 22
1399 [cited 2020 Oct 26];4. Available from:
1400 <https://www.ncbi.nlm.nih.gov/pmc/articles/PMC1081565/>
- 1401 113. Bando H, Okado K, Guelbeogo WM, Badolo A, Aonuma H, Nelson B, et al. Intra-specific
1402 diversity of *Serratia marcescens* in *Anopheles* mosquito midgut defines *Plasmodium*
1403 transmission capacity. *Scientific Reports*. 2013 Apr 10;3(1):1–9.
- 1404 114. Cirimotich CM, Dong Y, Clayton AM, Sandiford SL, Souza-Neto JA, Mulenga M, et al.
1405 Natural Microbe-Mediated Refractoriness to *Plasmodium* Infection in *Anopheles*
1406 *gambiae*. *Science*. 2011 May 13;332(6031):855–8.
- 1407 115. Zhao H, Li G, Guo D, Wang Y, Liu Q, Gao Z, et al. Transcriptomic and metabolomic
1408 landscape of the molecular effects of glyphosate commercial formulation on *Apis*
1409 *mellifera ligustica* and *Apis cerana cerana*. *Science of The Total Environment*. 2020
1410 Nov 20;744:140819.
- 1411 116. Benoit JB, Vigneron A, Broderick NA, Wu Y, Sun JS, Carlson JR, et al. Symbiont-induced
1412 odorant binding proteins mediate insect host hematopoiesis. *eLife* [Internet]. 2017
1413 [cited 2021 Feb 7];6. Available from:
1414 <https://www.ncbi.nlm.nih.gov/pmc/articles/PMC5231409/>
- 1415 117. Dzhavakhiya V, Voinova TM, Popletaeva S, Statsyuk N, Mikityuk O, Nazarova TA, et al.
1416 Some natural and synthetic compounds inhibiting the biosynthesis of aflatoxin B1
1417 and melanin in *Aspergillus flavus*. *SEL'SKOKHOZYAISTVENNAYA BIOLOGIA*. 2016
1418 Sep 1;51:533–42.
- 1419 118. Yu RJ, Scott EJV. N-(phosphonoalkyl)-amino acids, derivatives thereof and
1420 compositions and methods of use [Internet]. US7429575B2, 2008 [cited 2018 Jun
1421 19]. Available from:

- 1422 <https://patents.google.com/patent/US7429575B2/en?q=melanin&q=aminophosphoric+acid&q=A61Q19%2f02>
1423
- 1424 119. Seguin M-C, Babizhayev MA. Cosmetic composition useful notably for the skin
1425 whitening and melanogenesis inhibiting agent containing such a cosmetic
1426 composition [Internet]. US6280715B1, 2001 [cited 2018 Jun 19]. Available from:
1427 <https://patents.google.com/patent/US6280715B1/en>
- 1428 120. Jiang N, Sun N, Xiao D, Pan J, Wang Y, Zhu X. A copper-responsive factor gene CUF1 is
1429 required for copper induction of laccase in *Cryptococcus neoformans*. FEMS
1430 Microbiol Lett. 2009 Jul 1;296(1):84–90.
- 1431 121. Nenadis N, Wang L-F, Tsimidou M, Zhang H-Y. Estimation of Scavenging Activity of
1432 Phenolic Compounds Using the ABTS•+ Assay. J Agric Food Chem. 2004 Jul
1433 1;52(15):4669–74.
- 1434 122. Yu RJ, Scott EJV. Alpha hydroxyacids, alpha ketoacids and their use in treating skin
1435 conditions [Internet]. US4363815A, 1982 [cited 2019 Jun 8]. Available from:
1436 <https://patents.google.com/patent/US4363815A/en>
- 1437 123. Brauman KA, Flörke M, Mueller ND, Foley JA. Widespread Occurrence of Glyphosate
1438 and its Degradation Product (AMPA) in U.S. Soils, Surface Water, Groundwater, and
1439 Precipitation, 2001-2009. AGU Fall Meeting Abstracts. 2011 Dec 1;44:H44A-08.
- 1440 124. Hallmann CA, Sorg M, Jongejans E, Siepel H, Hofland N, Schwan H, et al. More than 75
1441 percent decline over 27 years in total flying insect biomass in protected areas. PLoS
1442 ONE. 2017;12(10):e0185809.
- 1443 125. Jarvis B. The Insect Apocalypse Is Here. The New York Times [Internet]. 2018 Nov 27
1444 [cited 2020 May 6]; Available from:
1445 <https://www.nytimes.com/2018/11/27/magazine/insect-apocalypse.html>
- 1446 126. Montgomery GA, Dunn RR, Fox R, Jongejans E, Leather SR, Saunders ME, et al. Is the
1447 insect apocalypse upon us? How to find out. Biological Conservation. 2020 Jan
1448 1;241:108327.
- 1449 127. Cardoso P, Leather SR. Predicting a global insect apocalypse. Insect Conservation and
1450 Diversity. 2019;12(4):263–7.
- 1451 128. Saunders ME, Janes JK, O’Hanlon JC. Moving On from the Insect Apocalypse Narrative:
1452 Engaging with Evidence-Based Insect Conservation. BioScience. 2020 Jan 1;70(1):80–
1453 9.
- 1454 129. Rosenheim JA, Ward PS. Insect diversity over 36 years at a protected Sierra Nevada
1455 (California) site: towards an evaluation of the insect apocalypse hypothesis.
1456 Ecological Entomology [Internet]. [cited 2020 Oct 25];n/a(n/a). Available from:
1457 <https://onlinelibrary.wiley.com/doi/abs/10.1111/een.12888>

- 1458 130. Saunders ME. Ups and downs of insect populations. *Nature Ecology & Evolution*.
1459 2019 Dec;3(12):1616–7.
- 1460 131. Cornet S, Gandon S, Rivero A. Patterns of phenoloxidase activity in insecticide
1461 resistant and susceptible mosquitoes differ between laboratory-selected and wild-
1462 caught individuals. *Parasites Vectors*. 2013 Oct 31;6(1):315.
- 1463 132. Rodrigues J, Brayner FA, Alves LC, Dixit R, Barillas-Mury C. Hemocyte Differentiation
1464 Mediates Innate Immune Memory in *Anopheles gambiae* Mosquitoes. *Science*. 2010
1465 Sep 10;329(5997):1353–5.
- 1466 133. Schindelin J, Arganda-Carreras I, Frise E, Kaynig V, Longair M, Pietzsch T, et al. Fiji: an
1467 open-source platform for biological-image analysis. *Nature Methods*. 2012
1468 Jul;9(7):676–82.
- 1469 134. Thompson PG, Smouse PE, Scofield DG, Sork VL. What seeds tell us about birds: a
1470 multi-year analysis of acorn woodpecker foraging movements. *Movement Ecology*.
1471 2014 Jun 23;2(1):12.
- 1472 135. Cornet S, Gandon S, Rivero A. Patterns of phenoloxidase activity in insecticide
1473 resistant and susceptible mosquitoes differ between laboratory-selected and wild-
1474 caught individuals. *Parasites & Vectors*. 2013 Oct 31;6(1):315.
- 1475 136. Schloss PD, Westcott SL, Ryabin T, Hall JR, Hartmann M, Hollister EB, et al.
1476 Introducing mothur: Open-Source, Platform-Independent, Community-Supported
1477 Software for Describing and Comparing Microbial Communities. *Appl Environ*
1478 *Microbiol*. 2009 Dec 1;75(23):7537–41.
- 1479 137. Chong J, Liu P, Zhou G, Xia J. Using MicrobiomeAnalyst for comprehensive statistical,
1480 functional, and meta-analysis of microbiome data. *Nature Protocols*. 2020
1481 Mar;15(3):799–821.
- 1482 138. Dhariwal A, Chong J, Habib S, King IL, Agellon LB, Xia J. MicrobiomeAnalyst: a web-
1483 based tool for comprehensive statistical, visual and meta-analysis of microbiome
1484 data. *Nucleic Acids Res*. 2017 03;45(W1):W180–8.
- 1485 139. Winder AJ, Harris H. New assays for the tyrosine hydroxylase and dopa oxidase
1486 activities of tyrosinase. *Eur J Biochem*. 1991 Jun 1;198(2):317–26.
- 1487 140. Maurya DK, Devasagayam TPA. Antioxidant and prooxidant nature of
1488 hydroxycinnamic acid derivatives ferulic and caffeic acids. *Food Chem Toxicol*. 2010
1489 Dec;48(12):3369–73.
- 1490 141. Therneau TM. *coxme: Mixed Effects Cox Models* [Internet]. 2020 [cited 2021 Feb 7].
1491 Available from: <https://CRAN.R-project.org/package=coxme>
- 1492

Figure 1

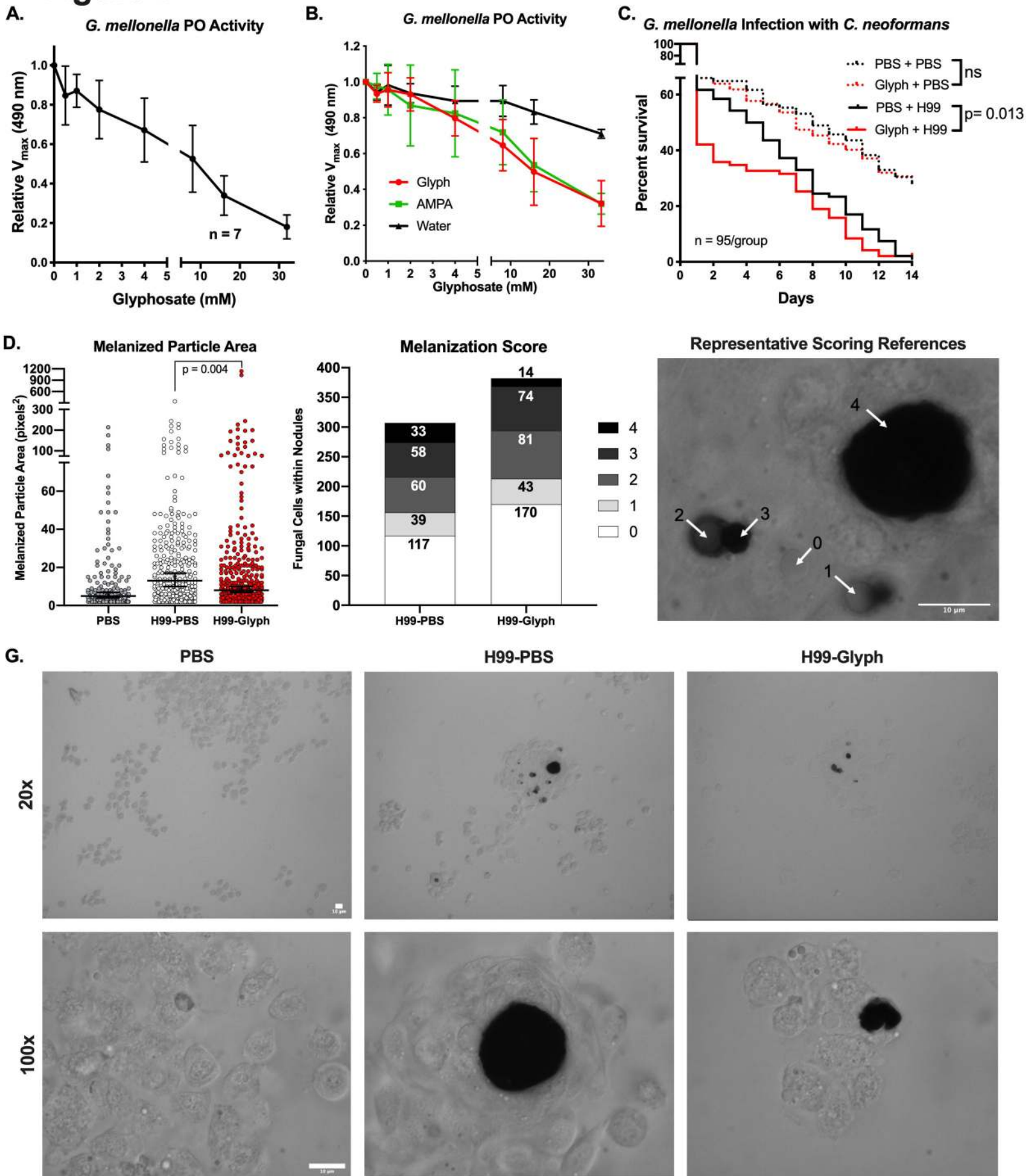
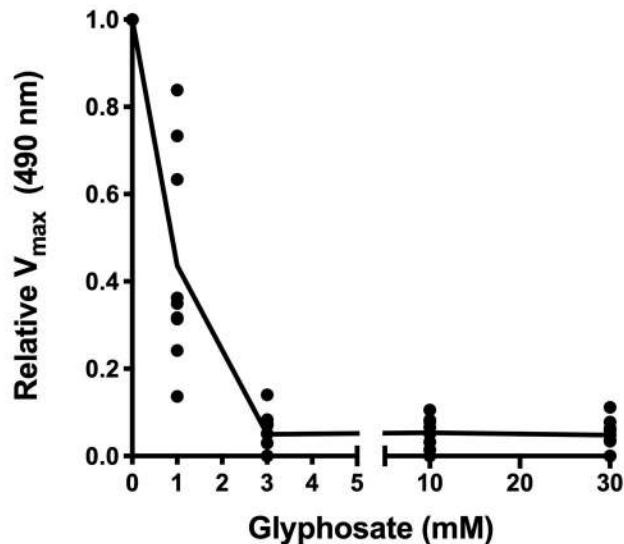


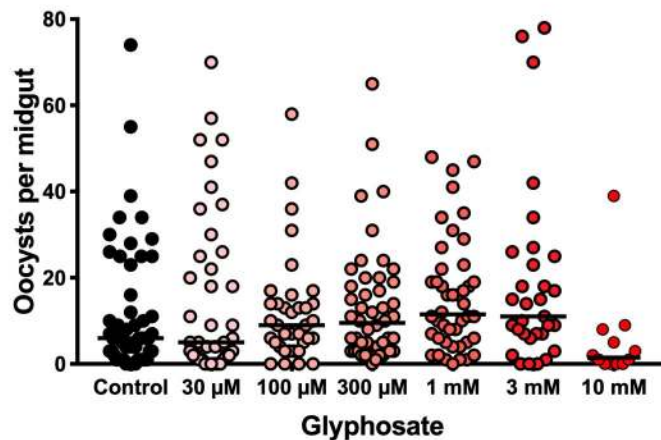
Figure 2

A *A. gambiae* Homogenate PO Activity

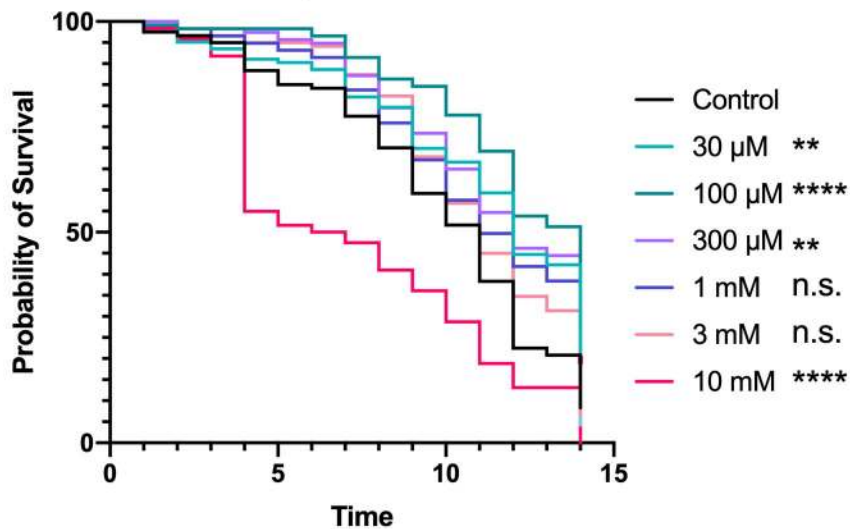


B *P. falciparum* Infection of *A. gambiae*

	n = 54	39	36	48	44	31	12
Median:	6	5	9	9.5	11.5	11	1.5
p-value:	—	0.708	0.233	0.178	0.016	0.038	0.045
Corrected p-value:	—	>0.99	>0.99	>0.99	0.11	0.19	0.32



C Mosquito Survival



D Cox Mixed Effect Model

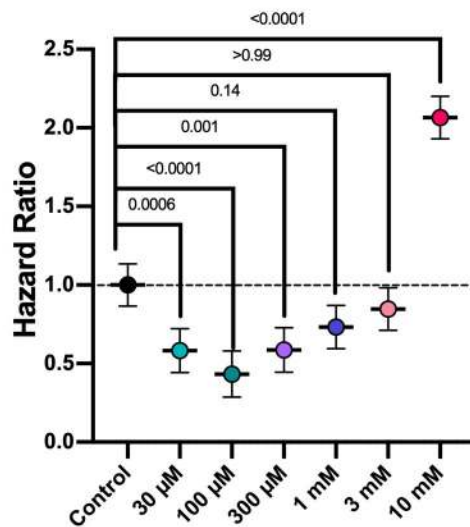
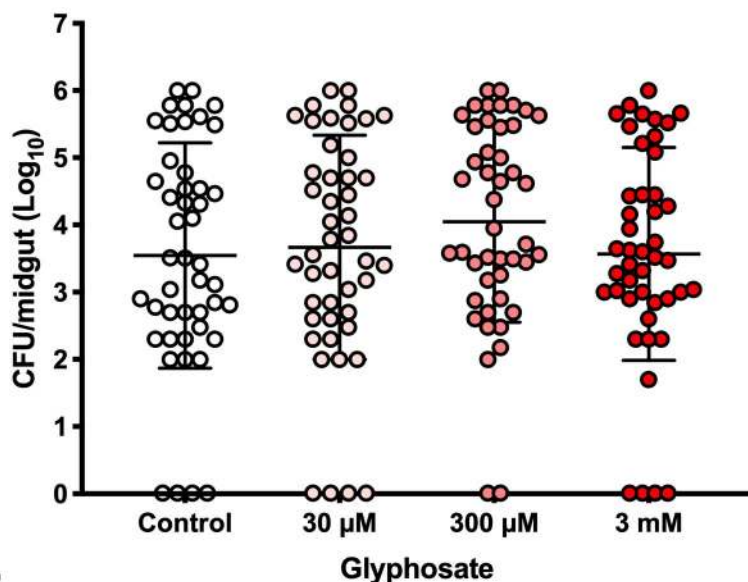


Figure 3

A Glyphosate and Mosquito Microbiome



B Glyphosate

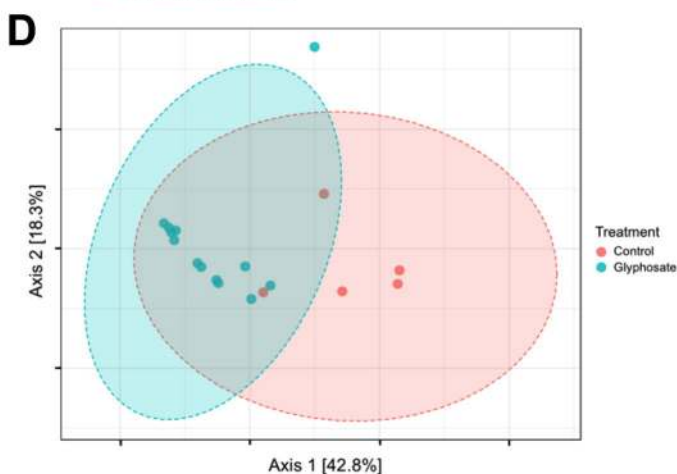
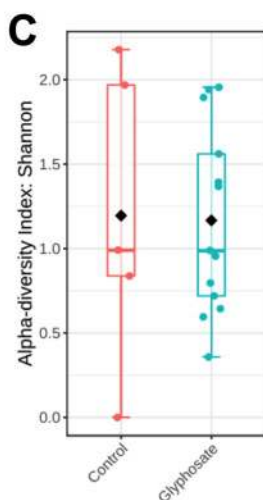
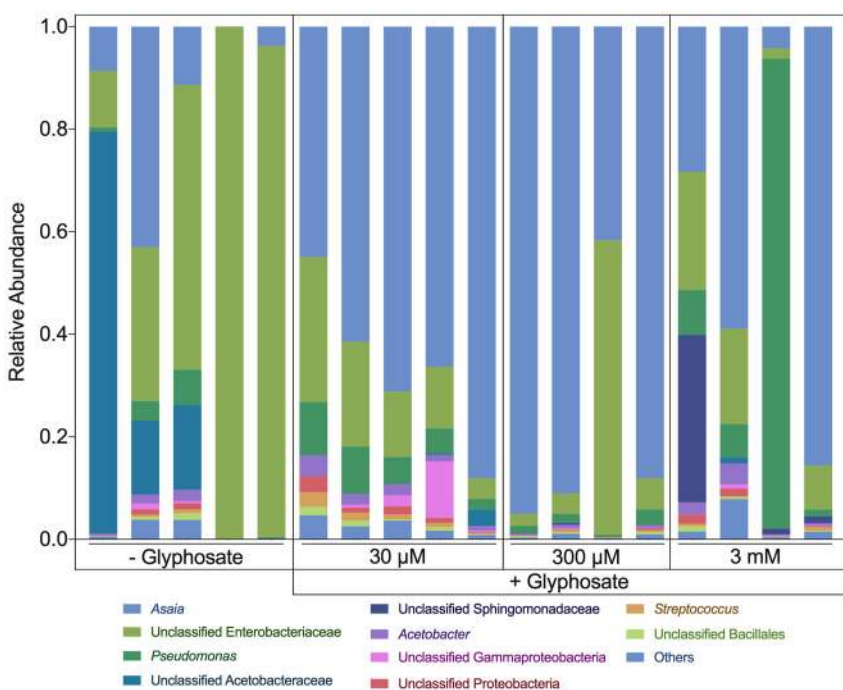
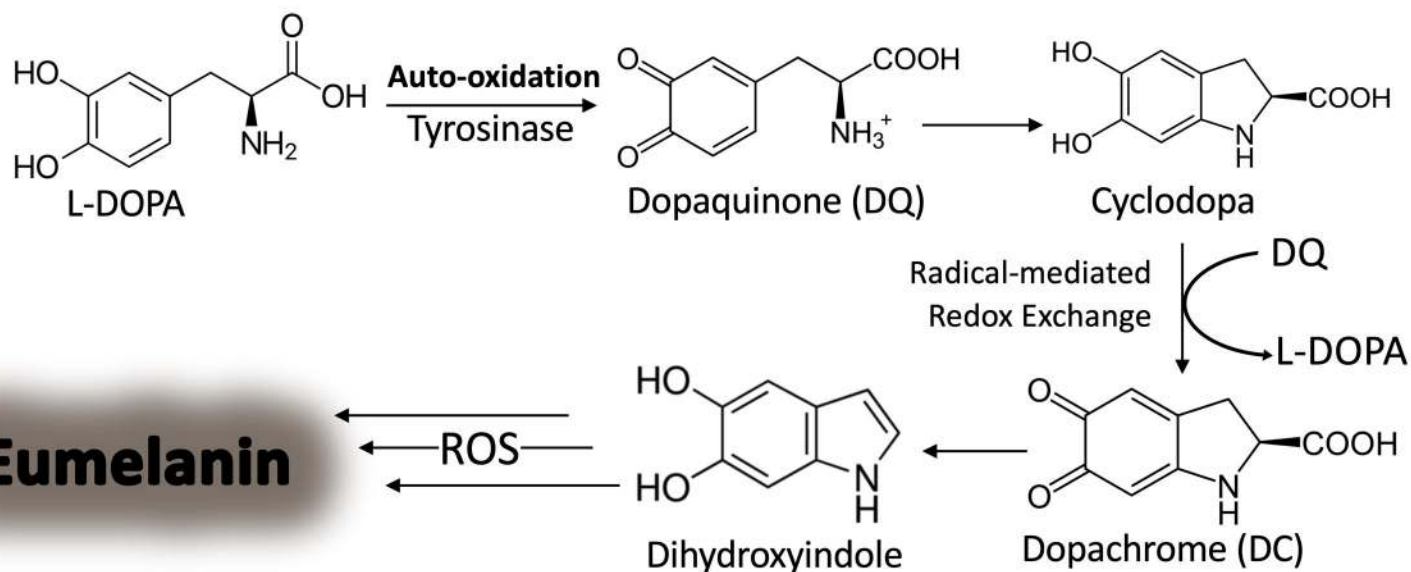
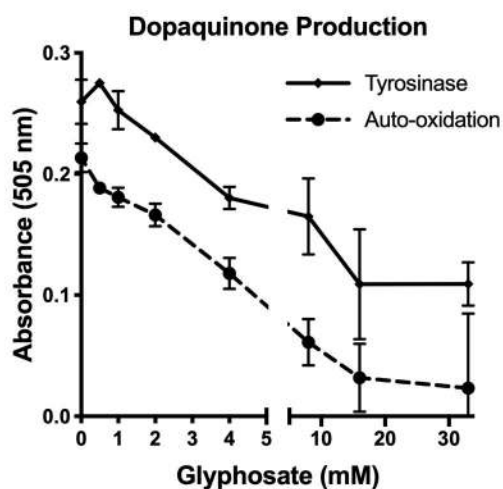


Figure 4

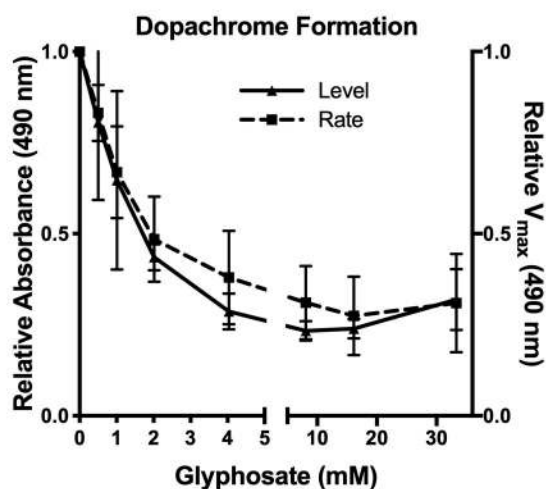
A



B



C



D

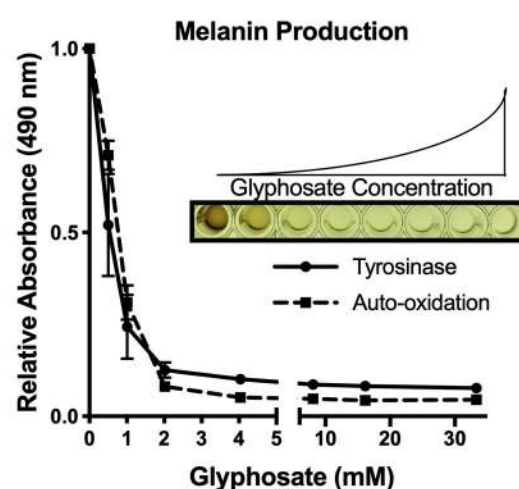


Figure 5

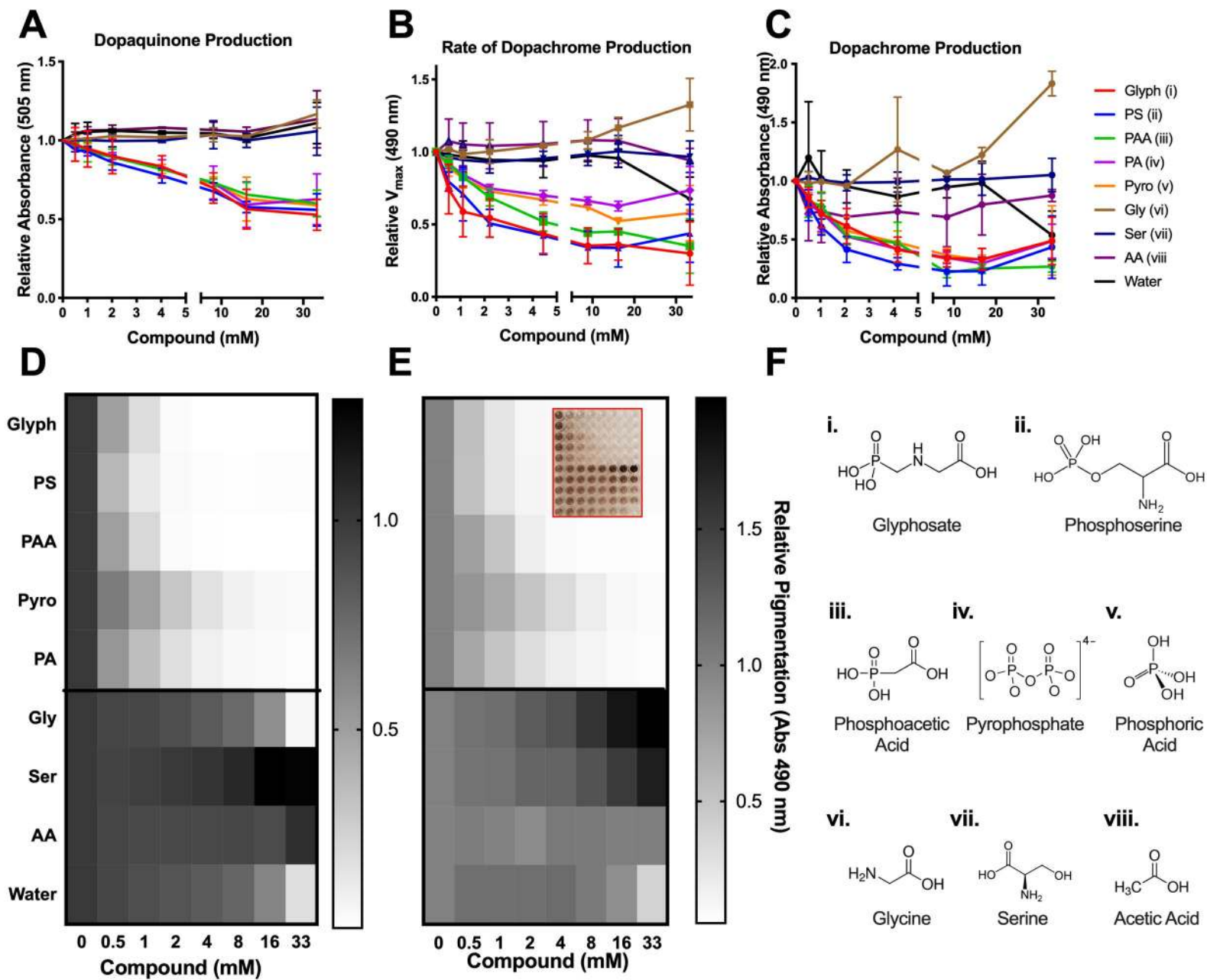
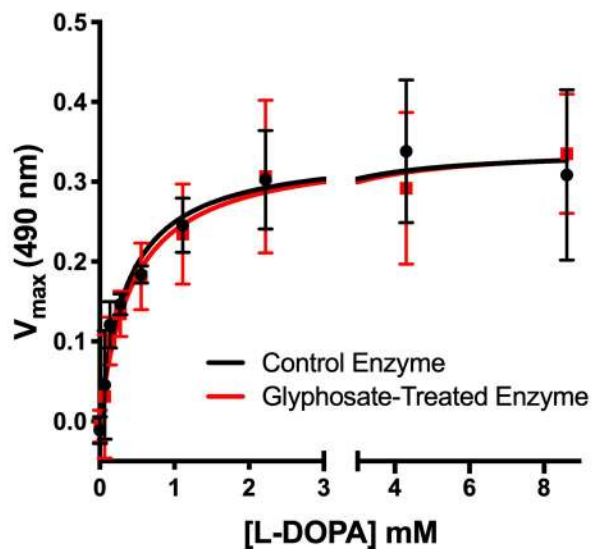
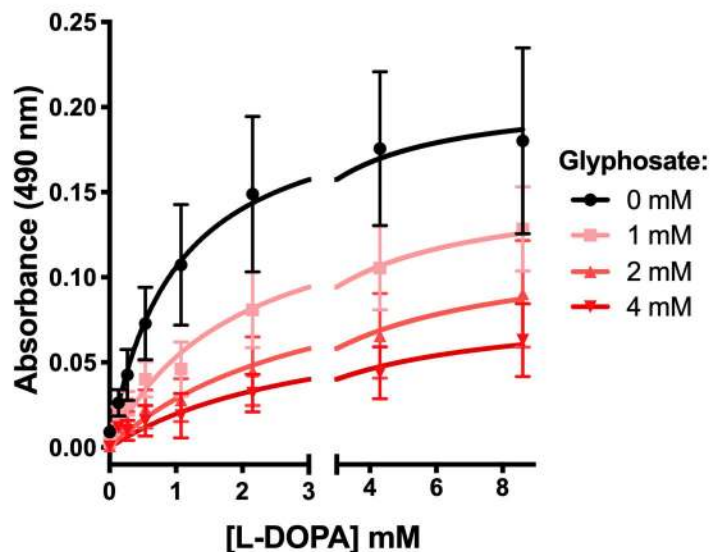


Figure 6

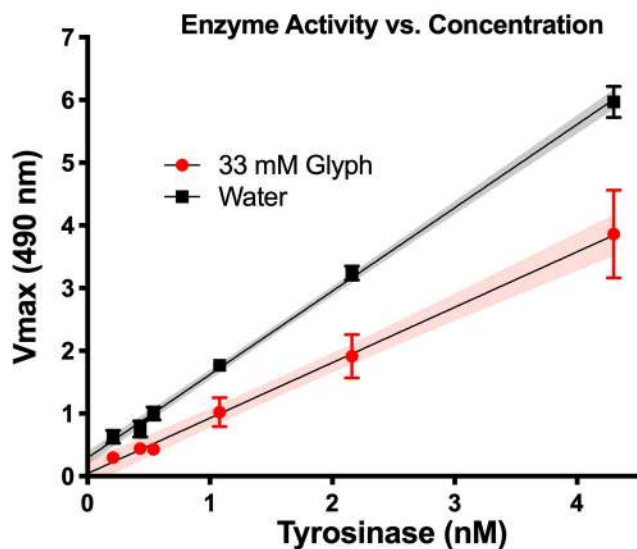
A



B



C



D

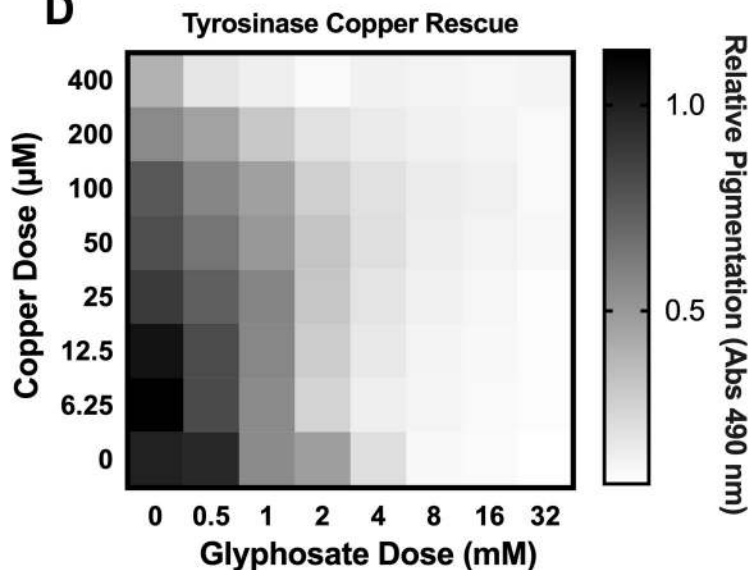
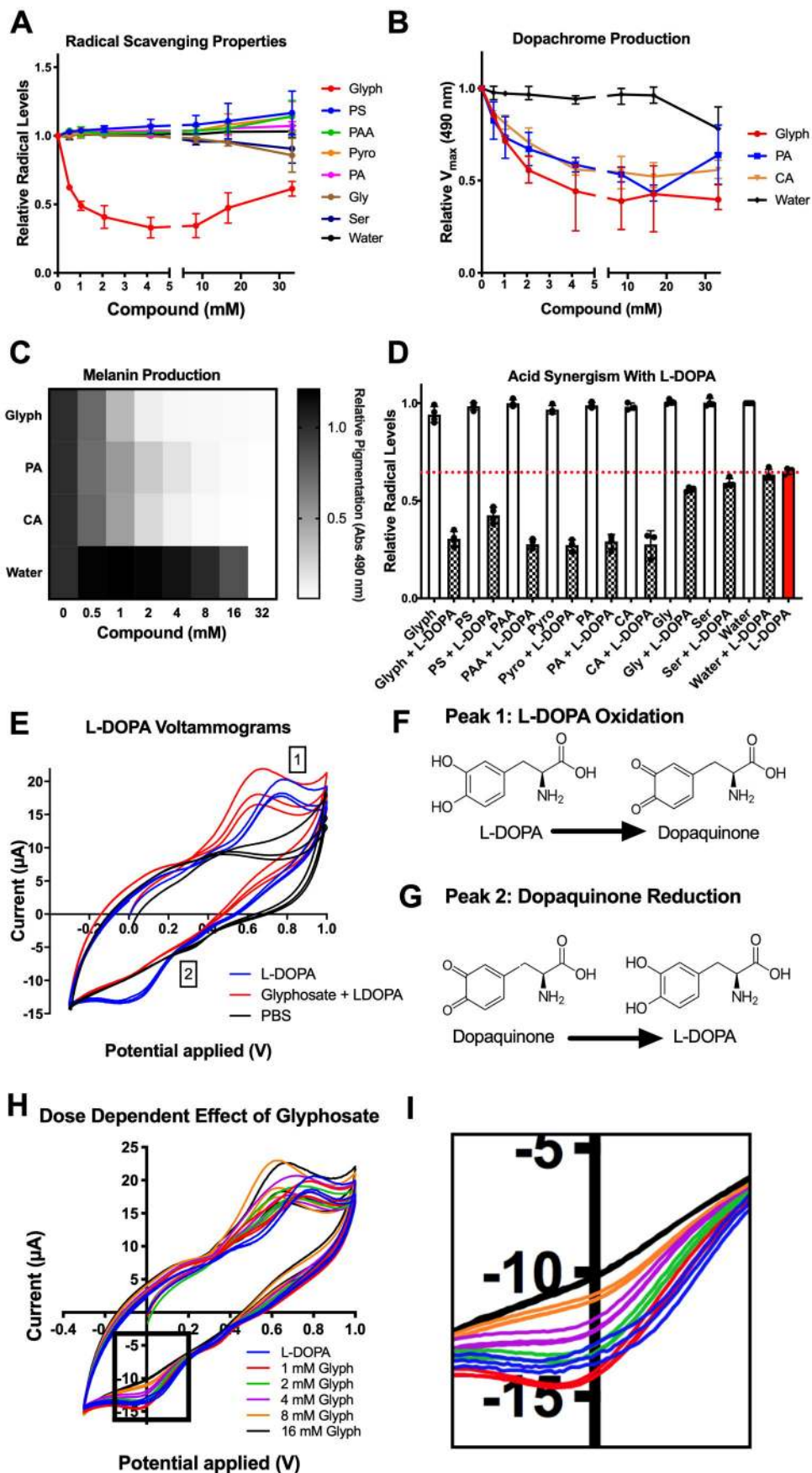
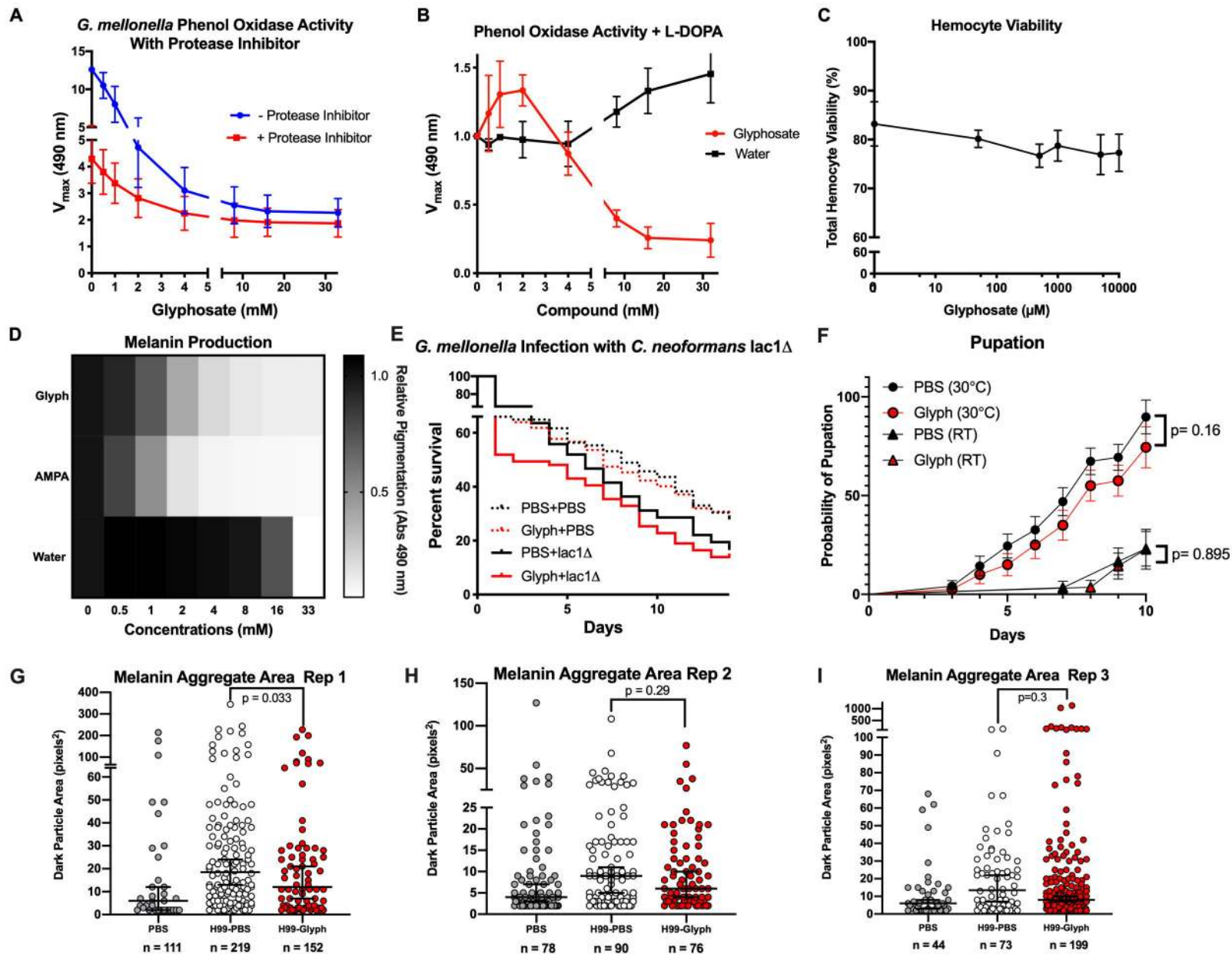


Figure 7



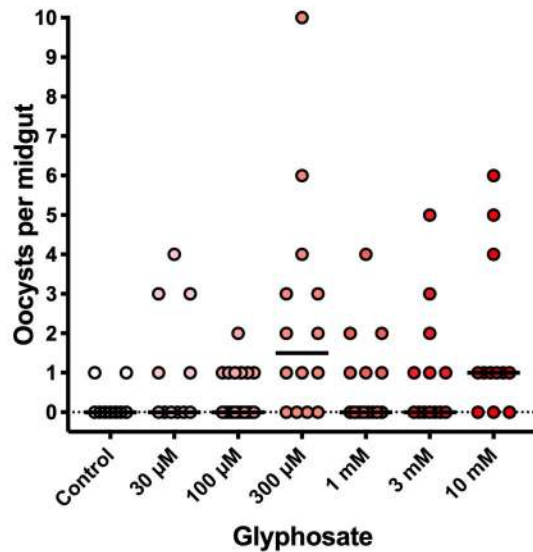
Supplementary Figure 1



Supplementary Figure 2

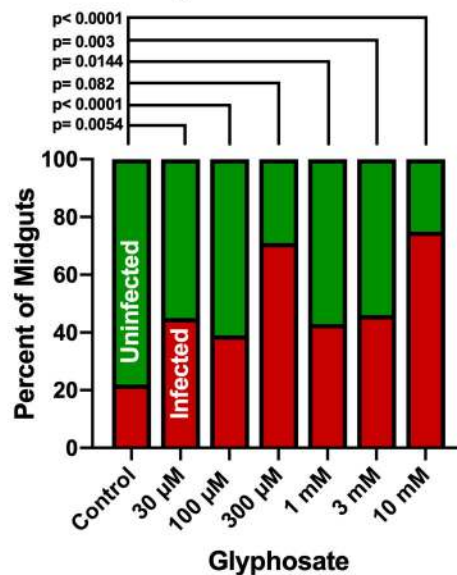
A.

Low *P. falciparum* Infection Burden



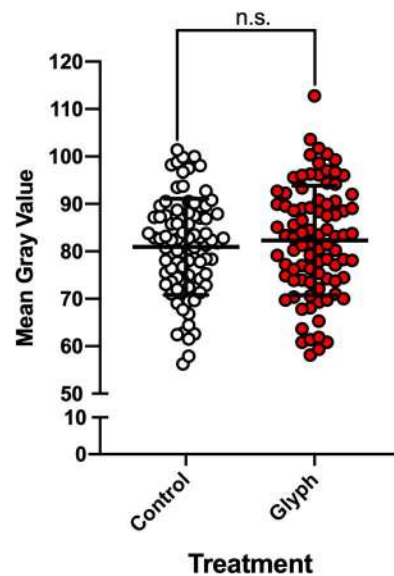
B.

Low *P. falciparum* Infection Prevalence



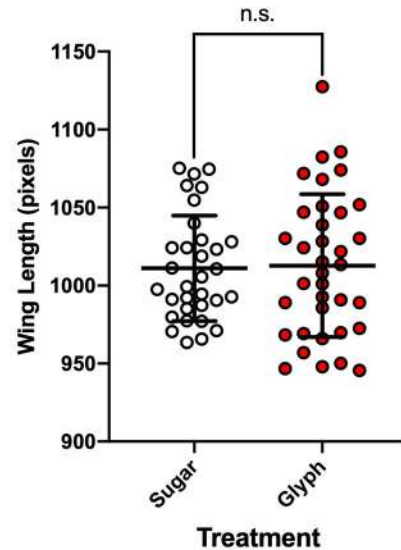
C.

Mosquito Cuticle Pigmentation



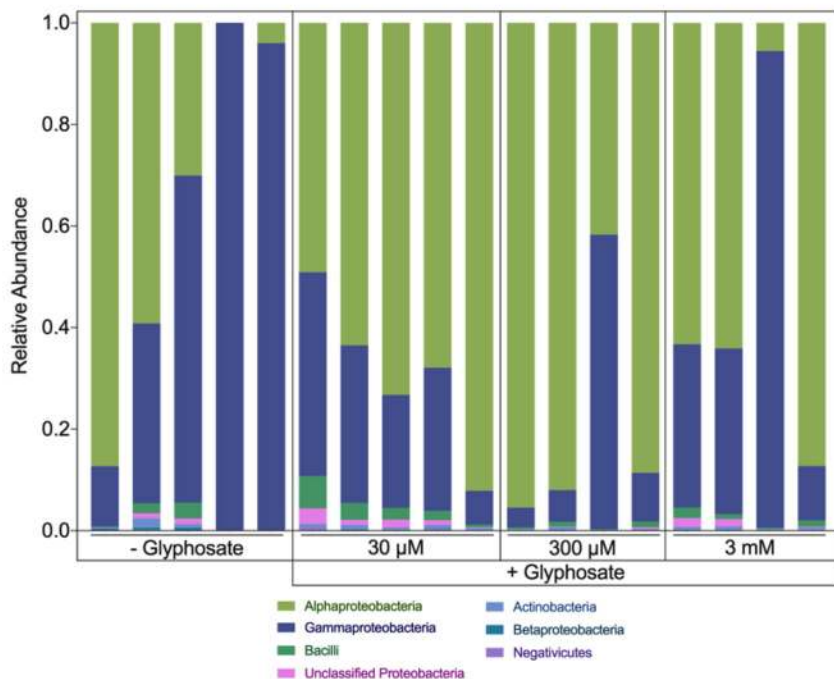
D.

Mosquito Wing Length



Supplementary Figure 3

A



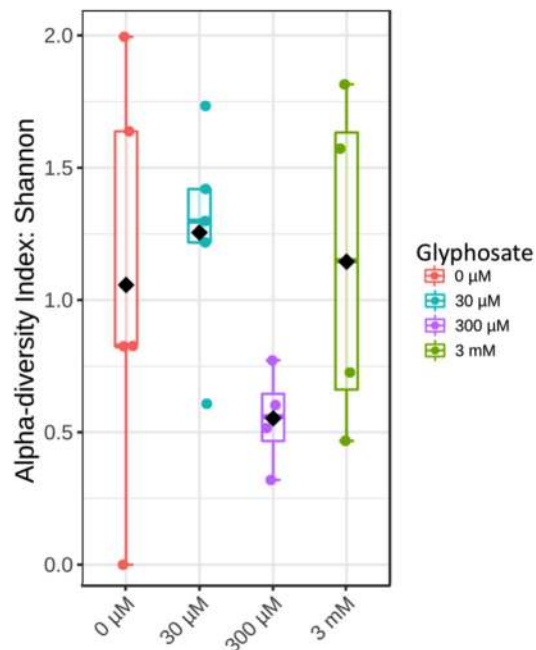
B

Class	[Glyphosate]			
	- Glyphosate	30 μM	300 μM	3 mM
Actinobacteria	0.0058	0.005642	0.002504	0.00476
Alphaproteobacteria	0.45129705	0.6918657	0.7944112	0.5505296
Bacilli	0.01333963	0.0286482	0.006664	0.0113333
Betaproteobacteria	0.0041215	0.000844	0.0001336	0.000471
Gammaproteobacteria	0.51917302	0.2566697	0.1942569	0.423504
Negativicutes	0.00042991	0.0025054	0.0003698	0.0005008
Unclassified Proteobacteria	0.00580703	0.013826	0.00166	0.0088853

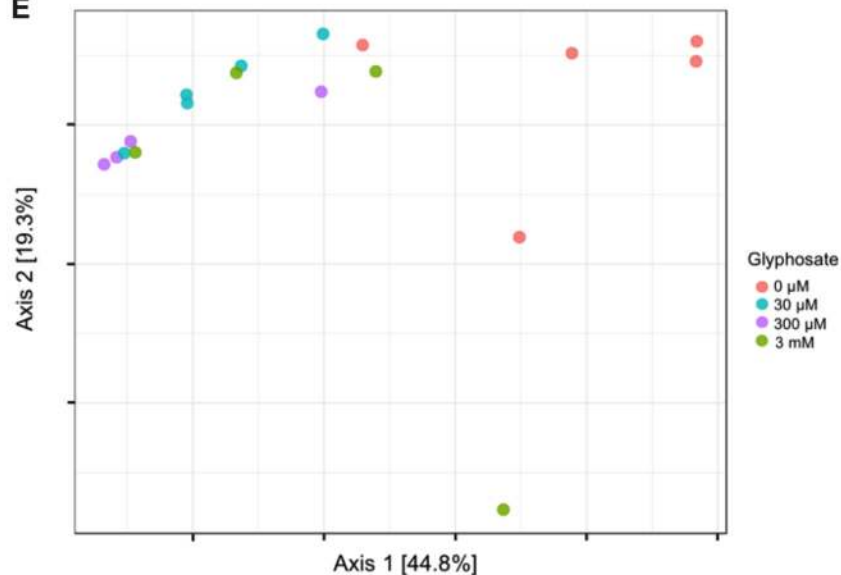
C

Genus	[Glyphosate]			
	- Glyphosate	30 μM	300 μM	3 mM
Asaia	0.1336578	0.664002	0.789541	0.442692
Unclassified Enterobacteriaceae	0.58495882	0.155066	0.174655	0.130596
Pseudomonas	0.02301406	0.063686	0.01635	0.271084
Unclassified Acetobacteraceae	0.21889554	0.006761	0.000116	0.002701
Unclassified Sphingomonadaceae	0	0	0.001265	0.087311
Acetobacter	0.00847871	0.021091	0.003683	0.01762
Unclassified Gammaproteobacteria	0.00343976	0.028129	0.000996	0.00285
Unclassified Proteobacteria	0.00464562	0.013806	0.001663	0.008885
Streptococcus	0.00243342	0.013	0.002609	0.003708
Unclassified Bacillales	0.0039732	0.007579	0.00253	0.004348
Others	0.0164868	0.026856	0.006594	0.02819

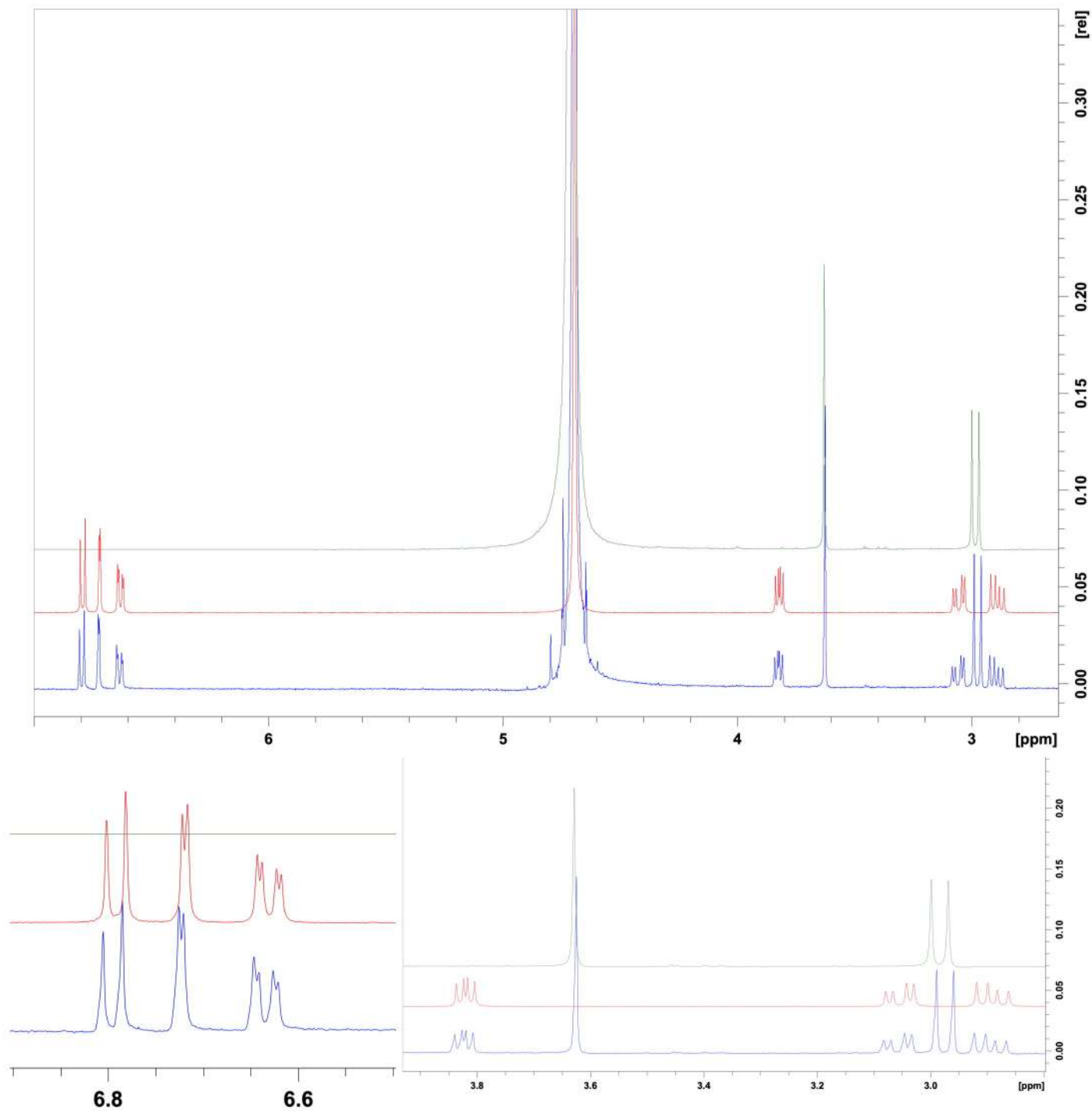
D



E

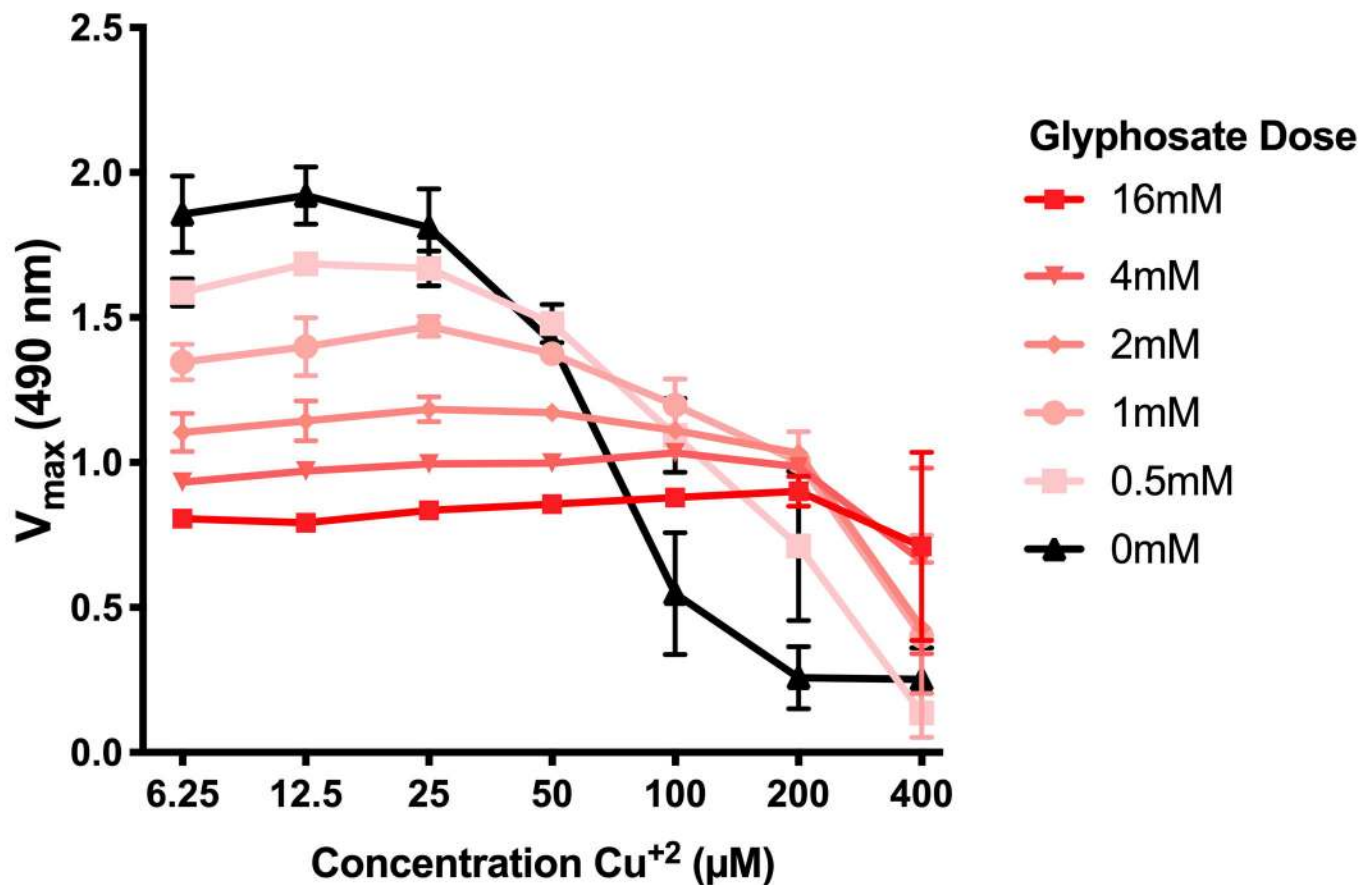


Supplementary Figure 4



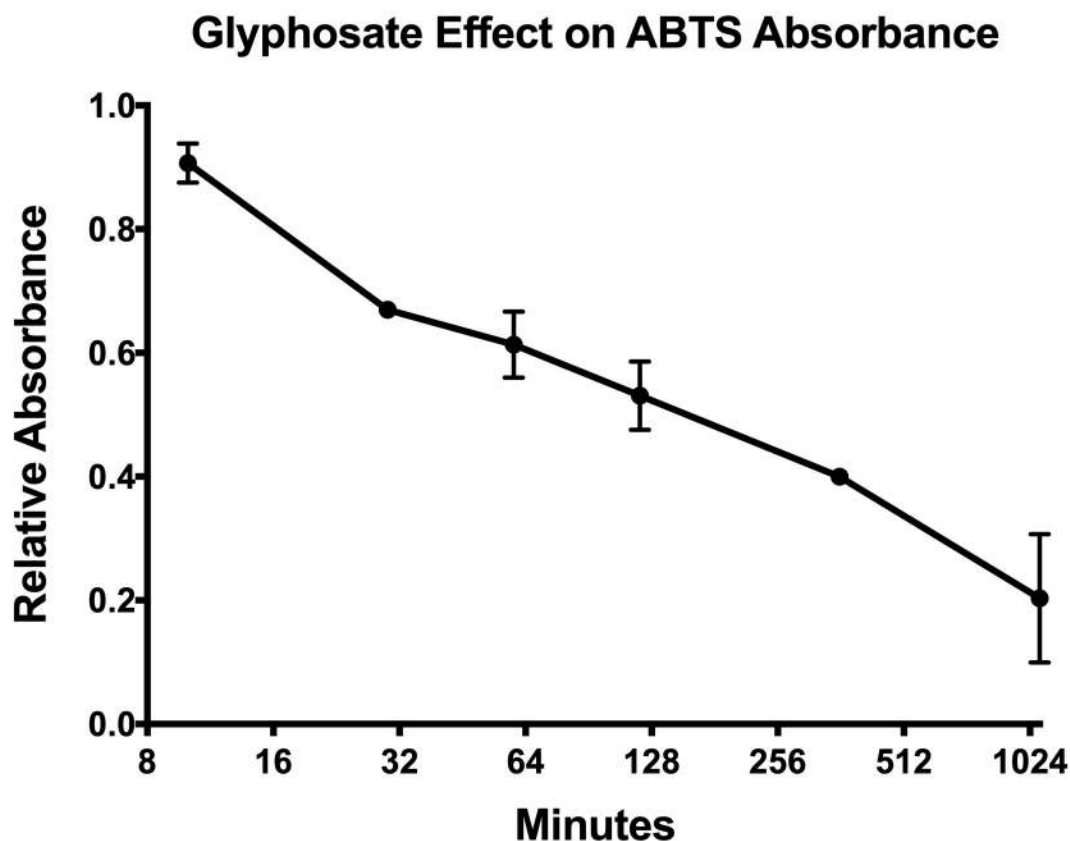
Supplementary Figure 5

Glyphosate "Buffers" Copper Ions



Supplementary Figure 6

A



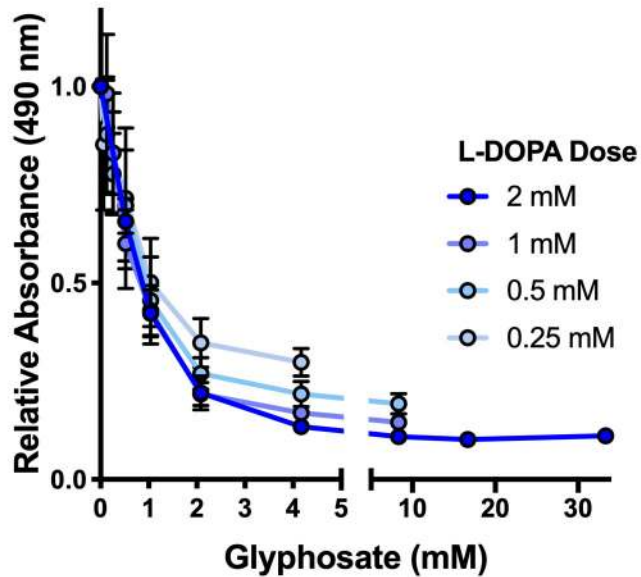
B

Compound	% Radical Quench-Compound Alone	% Radical Quench-Compound and L-DOPA	Synergy (Compared with L-DOPA alone)
Phosphoacetic Acid	0.020	72.288	0.483
Citric Acid	1.755	72.320	0.507
Phosphoric Acid	1.096	70.831	0.508
Pyrophosphate	3.320	72.675	0.526
Acetic Acid	1.327	64.155	0.565
Glyphosate	5.839	69.483	0.586
Phosphoserine	1.558	57.443	0.635
Glycine	-0.566	44.252	0.776
Serine	-0.386	40.808	0.846
Water	0.000	36.635	0.953
L-DOPA		34.904	1.000

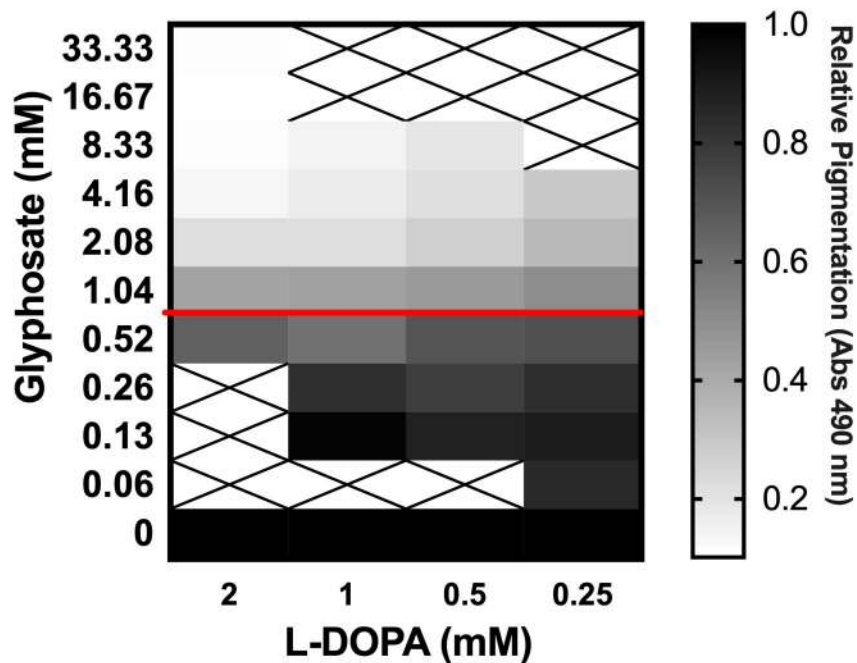
Supplementary Figure 7

A

Normalized Absorbance Values

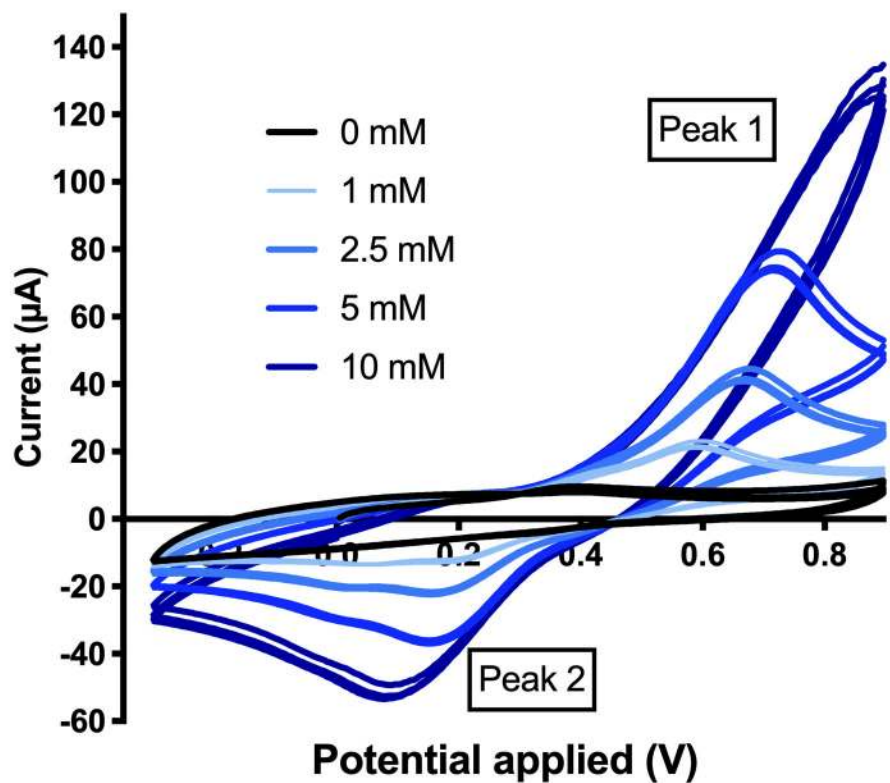


B

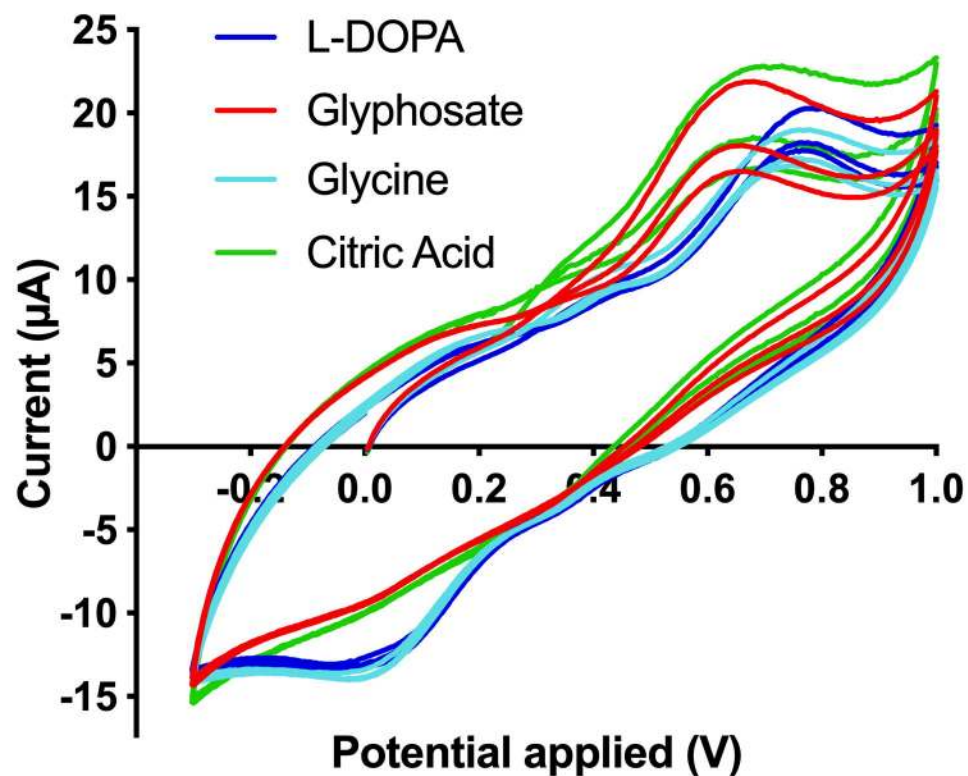


Supplementary Figure 8

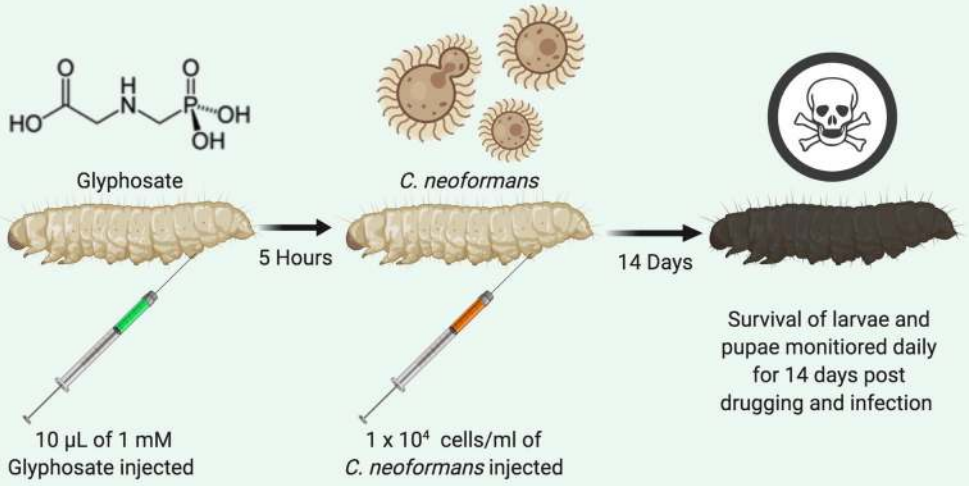
A L-DOPA Peak Validation



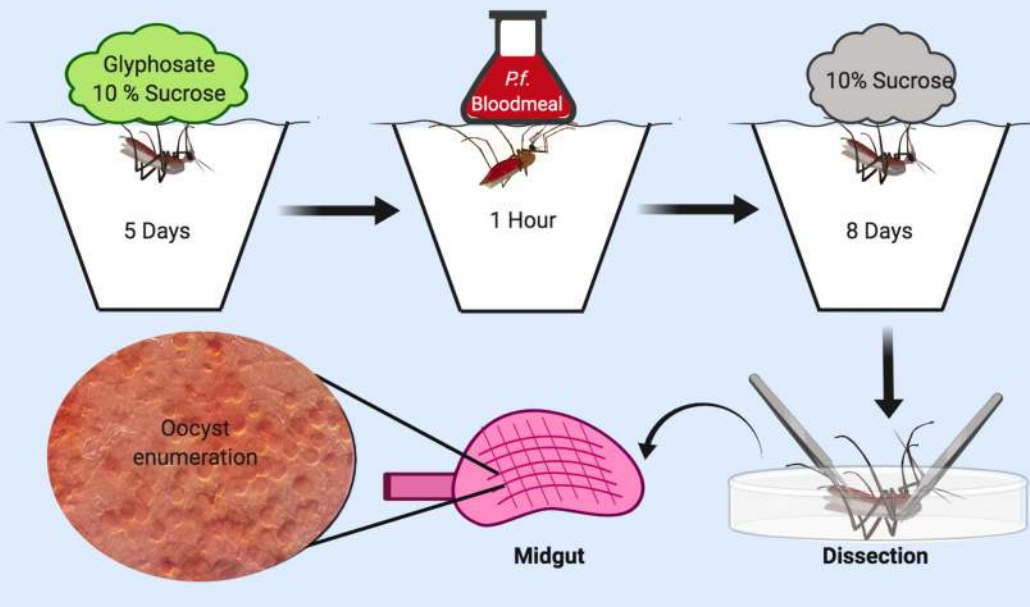
B Positive and Negative Inhibitor Controls



A



B



C

